MATERIALS EVALUATION REPORT

Materials Engineering Department

Rolls-Royce Corporation
450 S. Meridian Street
Indianapolis, Indiana
46225-1103, USA

REPORT NO.	REV.	PAGES
20FAE-033-PR	Initial	1 of 35

TITLE

METALLURGICAL INVESTIGATION OF A P_C SCROLL TO P_C FILTER TUBE ASSEMBLY, P/N 23065814, INSTALLED IN AN M250-C30P ENGINE, S/N CAE895054, OPERATED BY AIR EVAC EMS INC

PREPARED

Signatures on File

APPROVED

Signatures on File

IDENTIFICATION

Part Name:	Scroll to P_C Filter Tube Assembly
Part Number:	23065814
Part Serial Number:	Not Applicable
Part Time:	TSLSV: 114.9 hours, TSLT: 238.9 hours
Engine Model:	M250-C30P
Engine Serial Number:	CAE895054
FPA Number:	Not Applicable
FPD Number:	Not Applicable
Supplier:	Not Applicable
Vendor Code:	Not Applicable
User:	Air Evac EMS Inc
Removal Station:	Not Reported
Evaluations:	Failure Analysis
References:	AI-2020-019

1 Foreword

The subject engine was installed in a helicopter that reportedly made an emergency landing in a field. The helicopter reportedly sustained minor damage. The National Transportation Safety Board (NTSB) investigated the incident. The NTSB Investigator-in-Charge (IIC) reported a complete fracture of the P_C scroll to P_C air filter tube assembly (henceforth “tube”). A leak check was performed at the last maintenance 114.9 hours ago, and the tube was last removed 238.9 hours ago. Both parts of the tube and the attached air filter were sent to the Rolls-Royce Corporation Materials Laboratory in Indianapolis, IN for detailed metallurgical evaluation under the direction of the NTSB IIC.

2 Summary of Findings

2.1 The tube was fractured completely through at the toe of the weld between the tube and the air filter fitting. The fracture initiated in fatigue near the top location of the tube. Smearing damage on the surface precluded identification of any other modes of fracture.

2.2 The tube exhibited rub damage on the outer diameter surface of the elbow nearest the fracture surface. A red ribbed hose that was seen hanging in the engine bay near the fractured tube exhibited discoloration on the outer surface.

2.3 The height of the weld root reinforcement exceeded the component definition requirement.

3 Results and Discussion

Figure 1 shows a photograph provided to the author by the Rolls-Royce Air Safety Investigator showing a red ribbed hose adjacent to the elbow nearest the fracture on the fractured tube. The ribbed hose exhibited some dark discoloration in the area adjacent to the elbow surface.

The Rolls-Royce Air Safety Investigator was present for the unboxing of the engine hardware, shown in Figure 2. The box contained two bags, one containing most of the tube assembly and the other containing the welded fitting at the end of the tube assembly and the affixed air filter.

3.1 Visual and Non-Destructive Examination

The as-received condition of the fractured tube (except for the fitting end on the opposite side of the fracture) is shown in Figure 3. The tube fractured and separated at the weld adjacent to the air filter fitting. The fractured tube was compared to a newly manufactured tube, Figure 4, which did not reveal any obvious discrepancies in shape or dimension between the tubes. On the outer radius of the bend near the fracture surface, the event tube exhibited a flat spot surrounded by scuffing and patchy dark discoloration as shown in Figure 5. Detailed inspection of the area revealed several adjacent parallel oval-shaped dark patches near the flat spot as shown in Figure 6. The major dimension of the dark patches decreased in size progressing away from the flat spot. Both the flat spot and the oval-shaped dark patches were subjected to confocal laser scanning microscopy (CLSM). Figure 7 illustrates the flattened surface in the flat spot. CLSM revealed that the parallel adjacent oval-shaped dark patches were grooves in the surface of the tube measuring up to 0.0012 inch deep as shown in Figure 8.

Figure 9 shows a representative view of the weld on the opposite end of the tube from the fracture. In some locations the weld surface was slightly proud of the adjacent tube surface. The tube was sent to the Rolls-Royce Test Department for fluorescent penetrant inspection (FPI), which did not reveal any anomalies.

The as-received condition of the weld and fitting side of the fractured tube and the attached air filter is shown in Figure 10. The filter housing outer diameter surface was covered in small, highly reflective shallow impressions. Figure 11 shows 90° rotated views of the weld adjacent to the fracture. The top dead center alignment on the fitting was approximately 180° away from the weld start/stop point. The fracture surface was relatively flat and oriented perpendicular to the axis of the tube, and was located at the toe of the weld adjacent to the fitting.

3.2 Fractography / Scanning Electron Microscope and Chemistry Examination

Figure 12 shows the fitting side fracture surface after it was cleaned with soap and water and ultrasonically agitated in acetone and methanol. The fracture surface exhibited macroscopic features consistent with fatigue radiating away from the outer diameter surface of the tube near the top alignment of the tube. The fracture features radiated through the tube wall thickness and circumferentially in both directions from this location. The fracture exhibited smearing damage in large areas elsewhere on the fracture surface. Figure 13 shows the tube side fracture surface after cleaning. It exhibited similar features to the mating fracture surface shown in Figure 12, but exhibited less macroscopic smearing damage.

Because both fracture surfaces exhibited smearing damage in different locations, both were examined in the scanning electron microscope (SEM) and images from both fracture surfaces are shown in this report. The top location on the fitting side fracture surface is shown in Figure 14, where the fracture features radiated away from an origin area on the outer diameter surface. Figure 15 shows optical and backscattered electron (compositional contrast mode) SEM images of the outer diameter surface of the weld adjacent to the origin area. The origin area was located further toward the tube side of the weld than the adjacent circumference (appearing slightly proud of the rest of the fracture surface in the optical image shown in Figure 15). The fracture propagated through the thickness at the top location as shown in Figure 16 and propagated circumferentially in both directions from the origin area as shown in Figure 17 and Figure 18 (images shown are on the tube side fracture surface). There was also an area where fracture features appeared to radiate towards the outer diameter and counterclockwise away from a smeared area adjacent to the inner diameter surface, as shown in Figure 19 (tube side fracture surface). As observed optically, much of the tube side fracture surface was smeared, including in an arc spanning from approximately 120° to 200° clockwise from the origin. A detailed representative image of the smearing damage on the fracture surfaces is shown in Figure 20. The smearing damage on the fracture surfaces precluded identification of any other modes of fracture from the fine fracture features.

The flat spot and adjacent parallel grooves on the outer radius of the bend were examined in the SEM and subjected to semi-quantitative energy dispersive x-ray spectroscopy (EDS) analysis. Figure 21 shows a backscattered electron SEM image of both areas, which appeared darker than the surrounding surface. EDS results revealed that both the flat spot and parallel grooves contained elevated amounts of oxygen and silicon, along with base metal constituents.

3.3 Metallography

A cross-section was prepared through the weld on the fitting side fracture at the approximate plane of the fatigue origin, as indicated in Figure 15. The cross-section was polished using typical procedures and etched using Stainless No. 2; the resultant cross-section is shown in Figure 22. The cross-section revealed the fatigue fracture was located at the toe of the weld, initiating at the approximate intersection of the weld heat affected zone (HAZ) and the weld metal of the tube as shown in Figure 23 and Figure 24. There were no material anomalies at the fatigue origin location, which was located at the transition in geometry at the toe of the weld. The fatigue fracture progressed approximately along the intersection between the HAZ and weld metal near the outer diameter surface before proceeding into the HAZ to the inner diameter surface at this plane of examination.

Detailed views showing the weld, HAZ, and base metal microstructures are shown in Figure 25 and Figure 26. The weld and base metal microstructures were both consistent with the materials required by the component definition. It could not be determined from the microstructure or EDS results whether the weld was integral or contained weld rod material, which is optional per the component definition.

Figure 27 shows the etched cross-section with several dimensions measured at the plane of the fatigue origin. Note that the tube wall thickness was approximated, measuring from the origin surface on the outer diameter side to the inner diameter wall. The tube wall thickness was measured to be approximately 0.027 inch, which met the component definition requirement. The fitting side wall thickness measured 0.032 inch, which met the component definition requirement. The height of the weld crown on the outer diameter measured 0.011 inch from the fitting side surface, which met the component definition maximum requirement. The height of the root reinforcement measured 0.018 inch from the inner diameter surface on the tube side, which exceeded the component definition maximum requirement. The height of the root reinforcement measured 0.015 inch from the inner diameter surface on the fitting side, which met the component definition maximum requirement. The tube and fitting had different wall thicknesses and thus exhibited some mismatch in alignment. There was no

component definition requirement for weld width; measurements are provided for information only. The width of the weld measured approximately 0.101 inch on the outer diameter (terminating at the fracture surface) and 0.081 inch on the inner diameter.

A metallographic cross-section was prepared through the flat spot on the outer radius of the bend and polished to examine plane 1 as indicated in Figure 6. The cross-section was subsequently polished further to plane 2 for examination of the parallel grooves. Figure 28 shows an overall view of the cross-section at plane 1, which revealed the previously-described flat spot was slightly concave at this plane of examination. There was no corresponding deformation of the inner diameter surface opposite the flat spot. Detailed inspection of the surface in the flat spot revealed an oxide layer on the surface and some distortion of the microstructure as shown in Figure 29. For comparison, the surface of the tube on both sides of the flat spot is shown in Figure 30, which also shows the representative microstructure found in the tube away from the surface. The microstructure was consistent with the material required by the component definition.

The mount was polished to plane 2 (Figure 6) and the resultant cross-section is shown in Figure 31. This section contained both the flat spot and the adjacent parallel grooves. In this plane of examination, the flat spot did not have any curvature, and there was no corresponding deformation on the inner diameter surface opposite either the flat spot or the grooves. The microstructure and oxide on the flat spot surface in this plane of examination was similar to that found in plane 1. A detailed view of the cross-section at the parallel grooves is shown in Figure 32, which revealed some oxides on the surface and some distortion of the microstructure when compared to the representative surface microstructures shown in Figure 30.

3.4 Chemistry

Semi-quantitative energy dispersive x-ray spectroscopy (EDS) analysis determined the fitting side base metal and weld metal were composed of the materials required by the component definition.

Semi-quantitative x-ray fluorescence (XRF) analysis determined the tube base metal was composed of the materials required by the component definition.

4 Revision History

Issue	Change Summary	Date
PR	Not applicable	08 Sep 2020

5 Figures and Tables

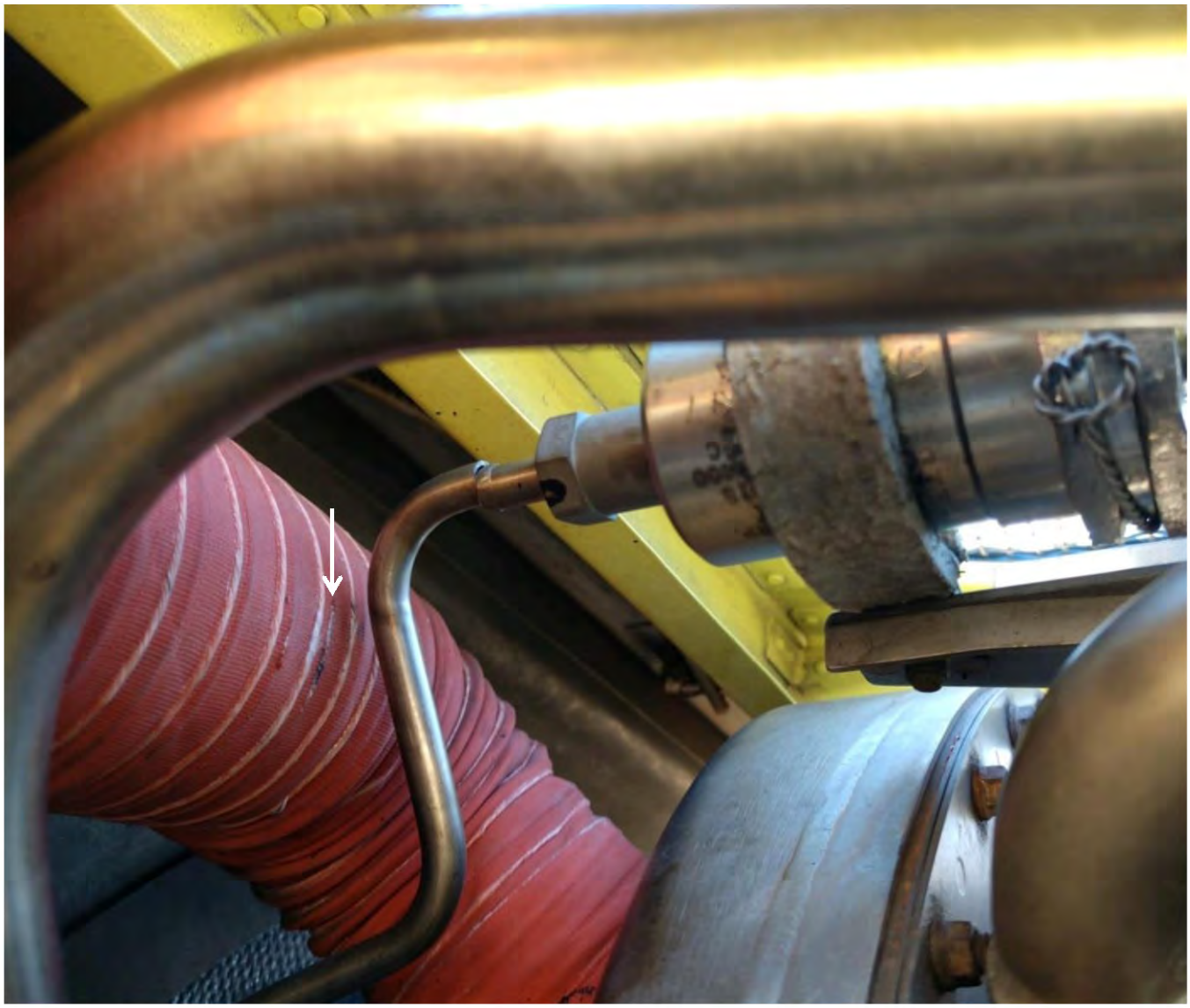

Figure 1. **Photograph showing the fractured P_C tube and the nearby ribbed hose that was adjacent to the elbow nearest the fracture. The hose surface exhibited some dark discoloration (white arrow). Photograph provided to the author by the Rolls-Royce Accident Investigation department. No scale provided.**

Figure 2. Shipping container (top) and the fractured tube (bottom left) and filter with remainder of tube still attached (bottom right) as received to the laboratory and removed from the packaging. No scale provided.

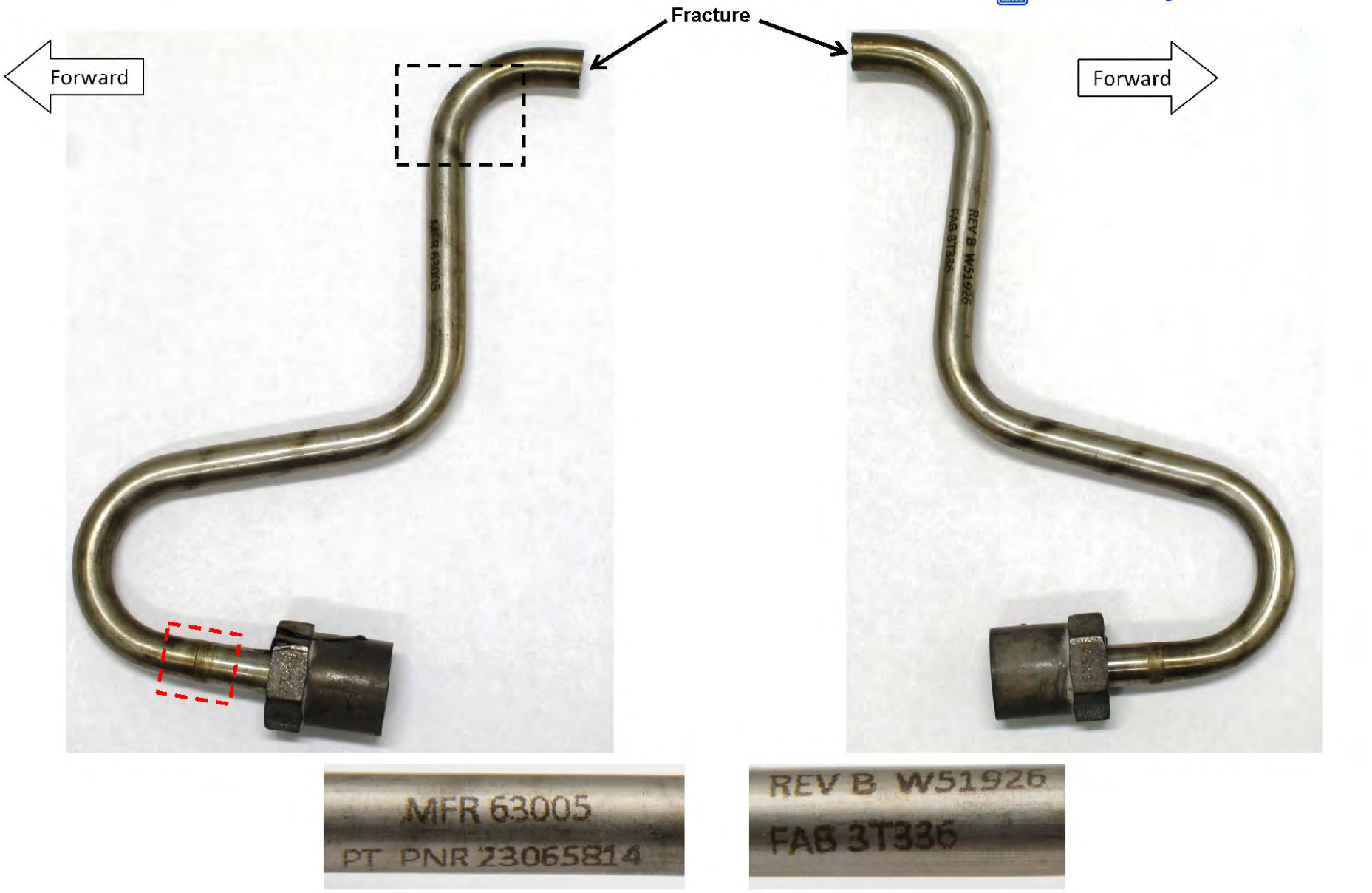

Figure 3. Overall views showing two sides of the fractured tube and detailed views showing the part markings on the tube (below). The black dashed boxed area is shown in Figure 5, and the red dashed boxed area is shown in Figure 9.

Figure 4. Comparison image showing the fracture tube (top) laid adjacent to a newly manufactured tube (bottom). There were no obvious discrepancies in the shape or dimensions between both tubes.

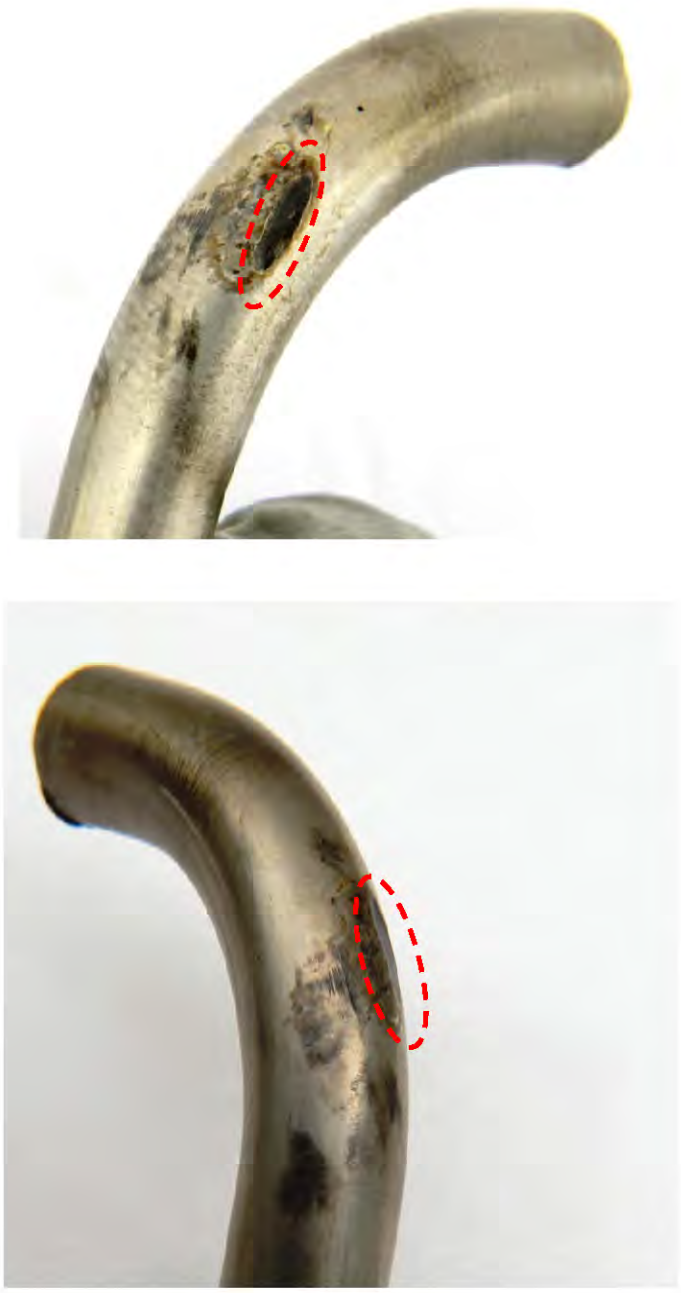

Figure 5. Detailed views showing the outer radius surface of the bend in the tube closest to the fracture. The tube exhibited a flat spot surrounded by patchy dark discoloration consistent with rub damage (red dashed outlined area).

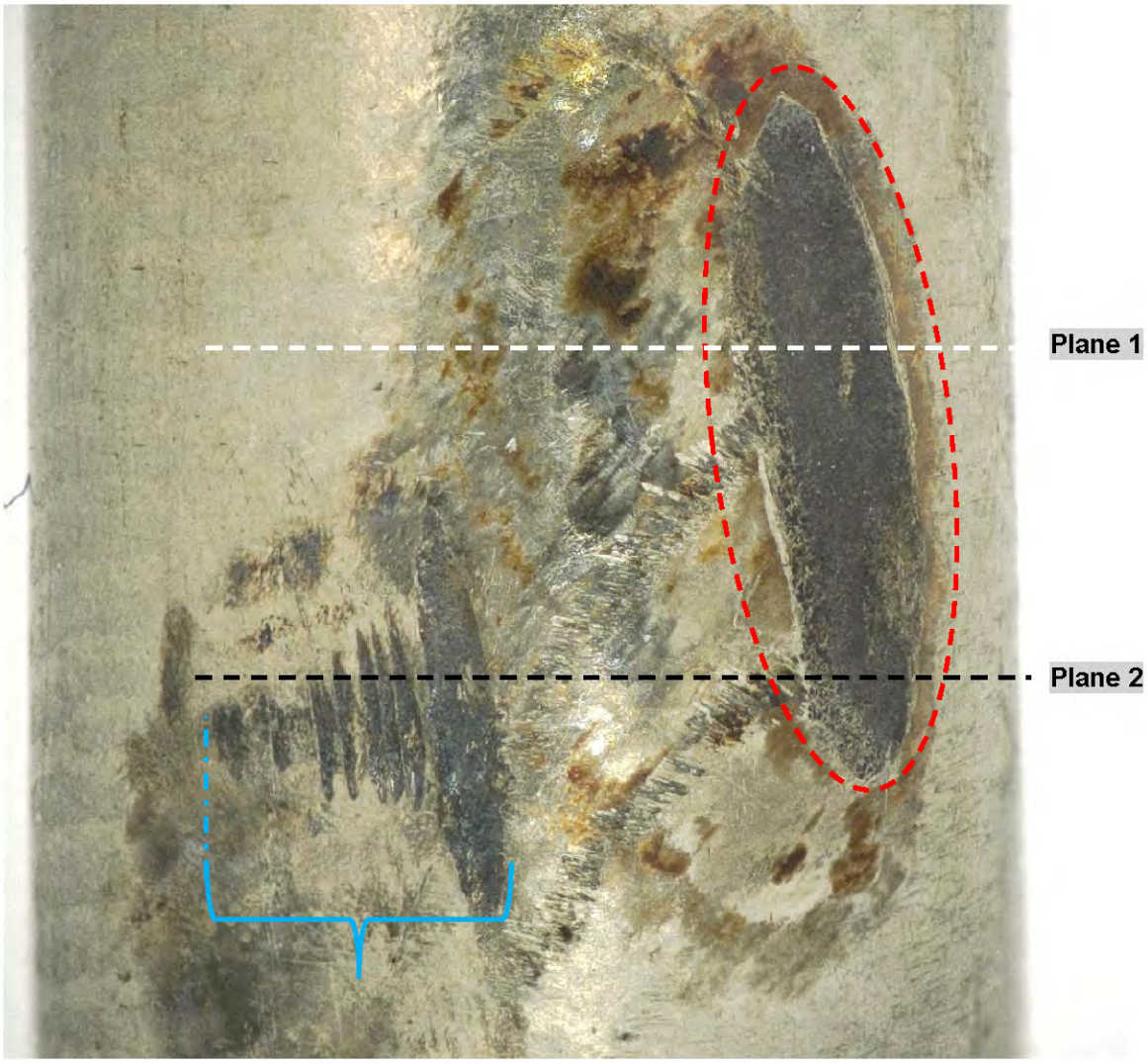

Figure 6. **Detailed view showing the flat spot (red dashed outlined area) and adjacent parallel oval-shaped dark patches (blue brace). The white and black dashed lines indicate planes of metallographic examination 1 and 2, respectively.**

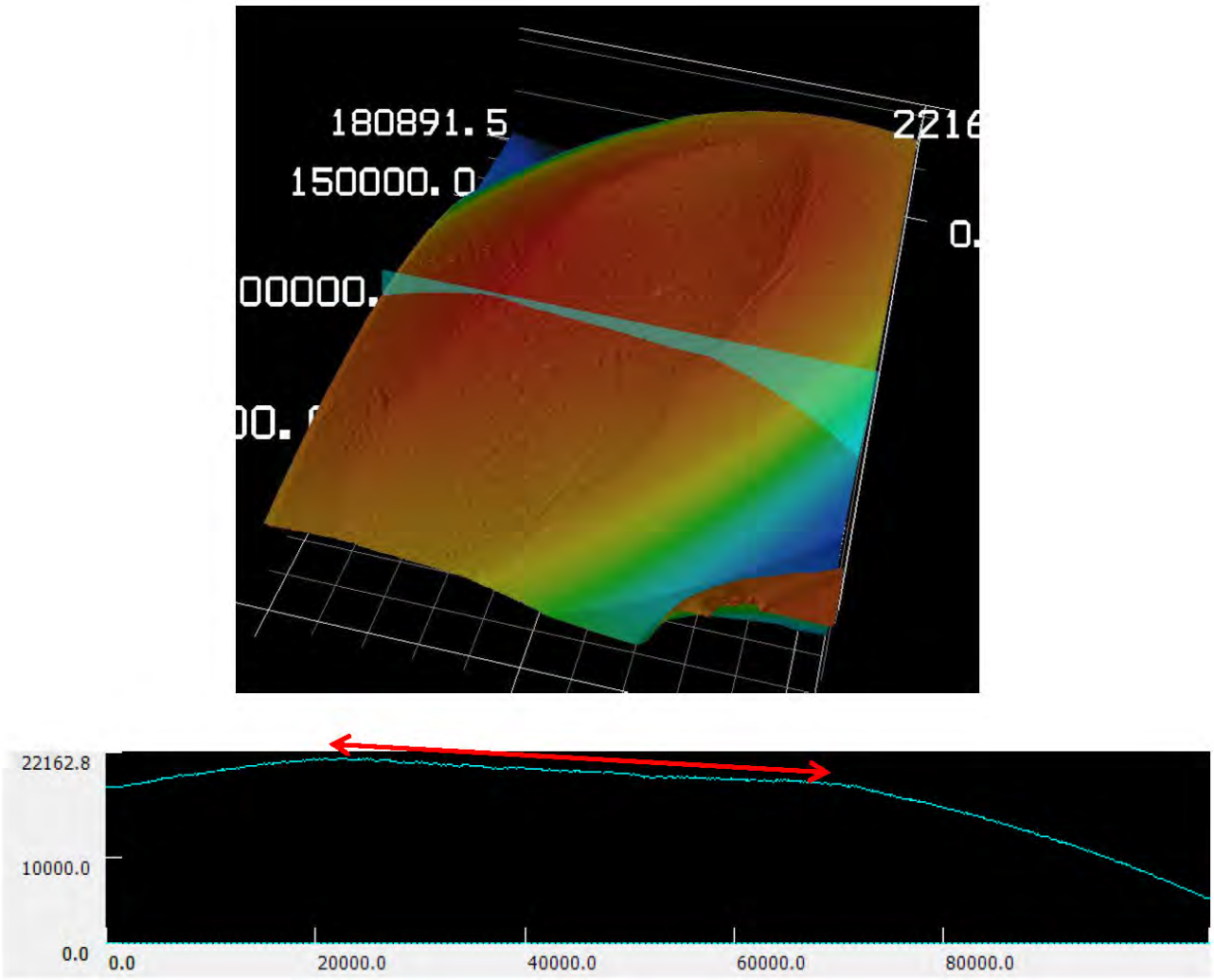

Figure 7. CLSM scan of the flat spot in the rub damaged area (top). A profile measurement taken through the rub damaged area illustrates the flattened surface (bottom, red arrow).

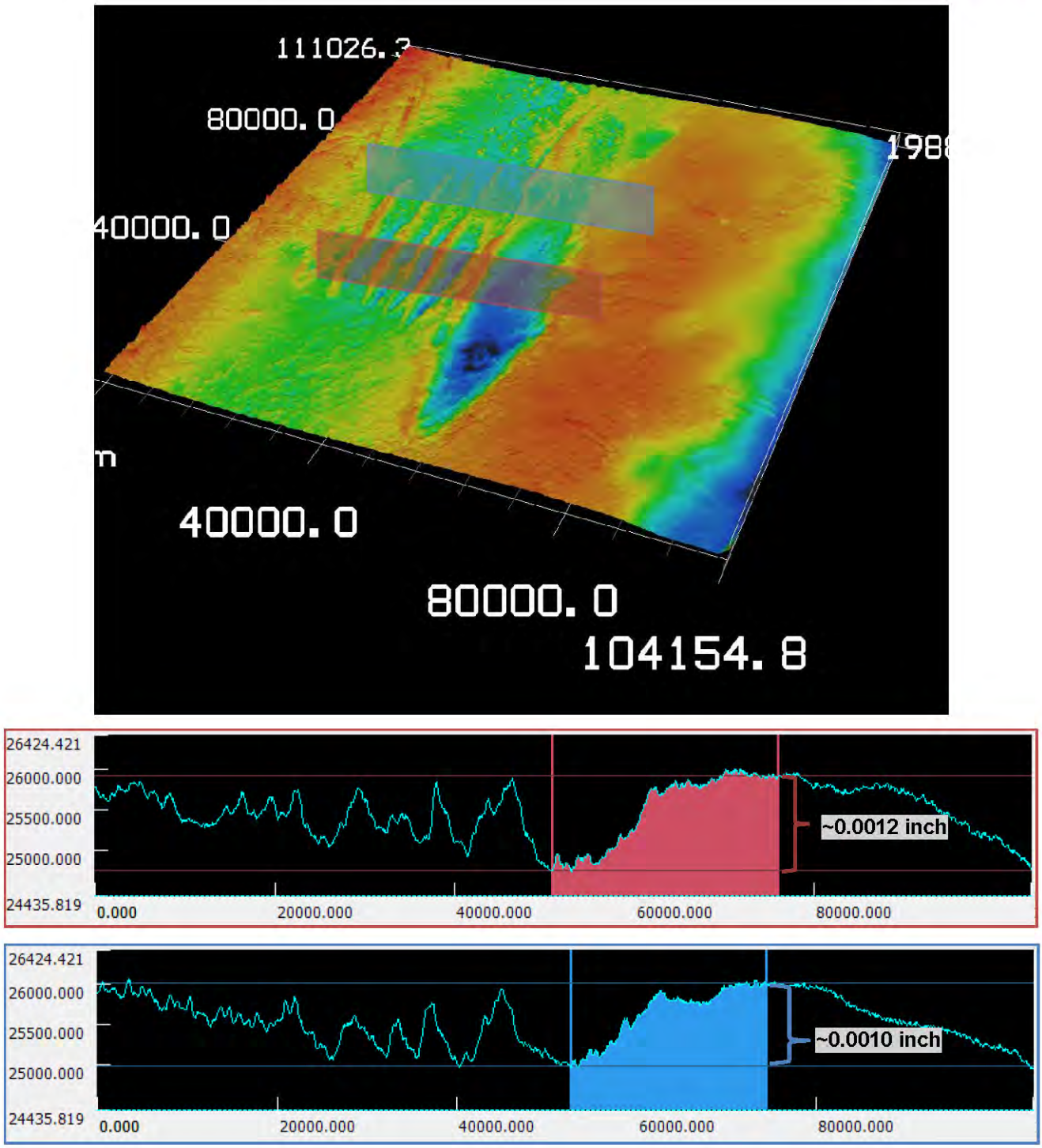

Figure 8. **CLSM scan of the adjacent oval-shaped dark patches in the rub damaged area (top). The as-manufactured curved surface of the tube was flattened in the CLSM scan. Profile measurements (bottom) taken through the area show the dark patches were adjacent grooves measuring up to 0.0012 inch deep in the largest and deepest of the grooves. The red and blue planes in the top image correspond to the locations of the profile measurements shown at bottom.**

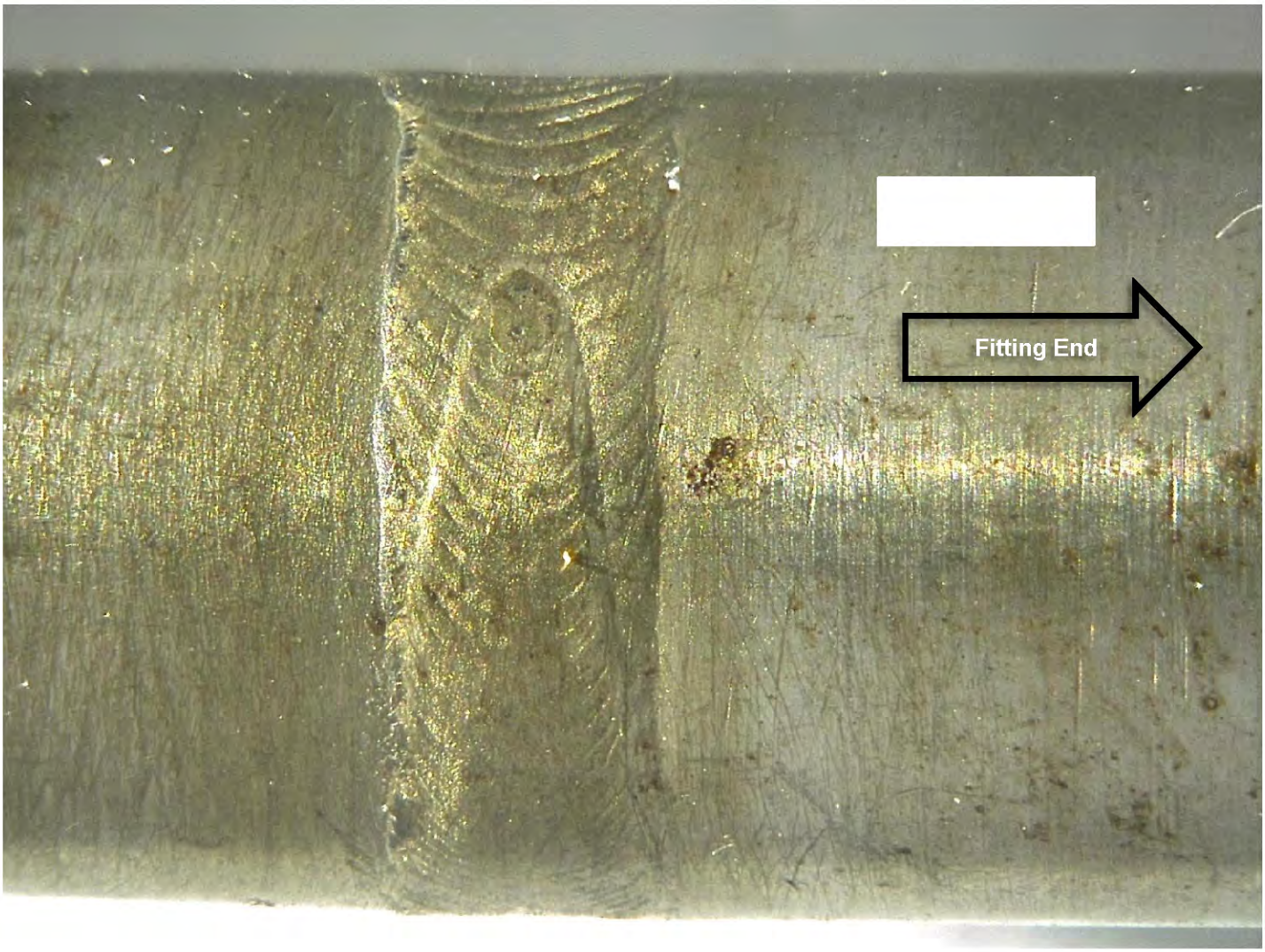

Figure 9. Detailed view showing the fitting weld at the opposite end of the tube from the fracture.

Figure 10. Overall view showing the compressor discharge air filter and the fractured tube (top). The surface of the filter was covered in bright, highly reflective small impressions consistent with gripping marks from a tool. The gripping marks on the outer diameter of the filter housing were present in the as-received condition. Divisions = 0.1 inch.

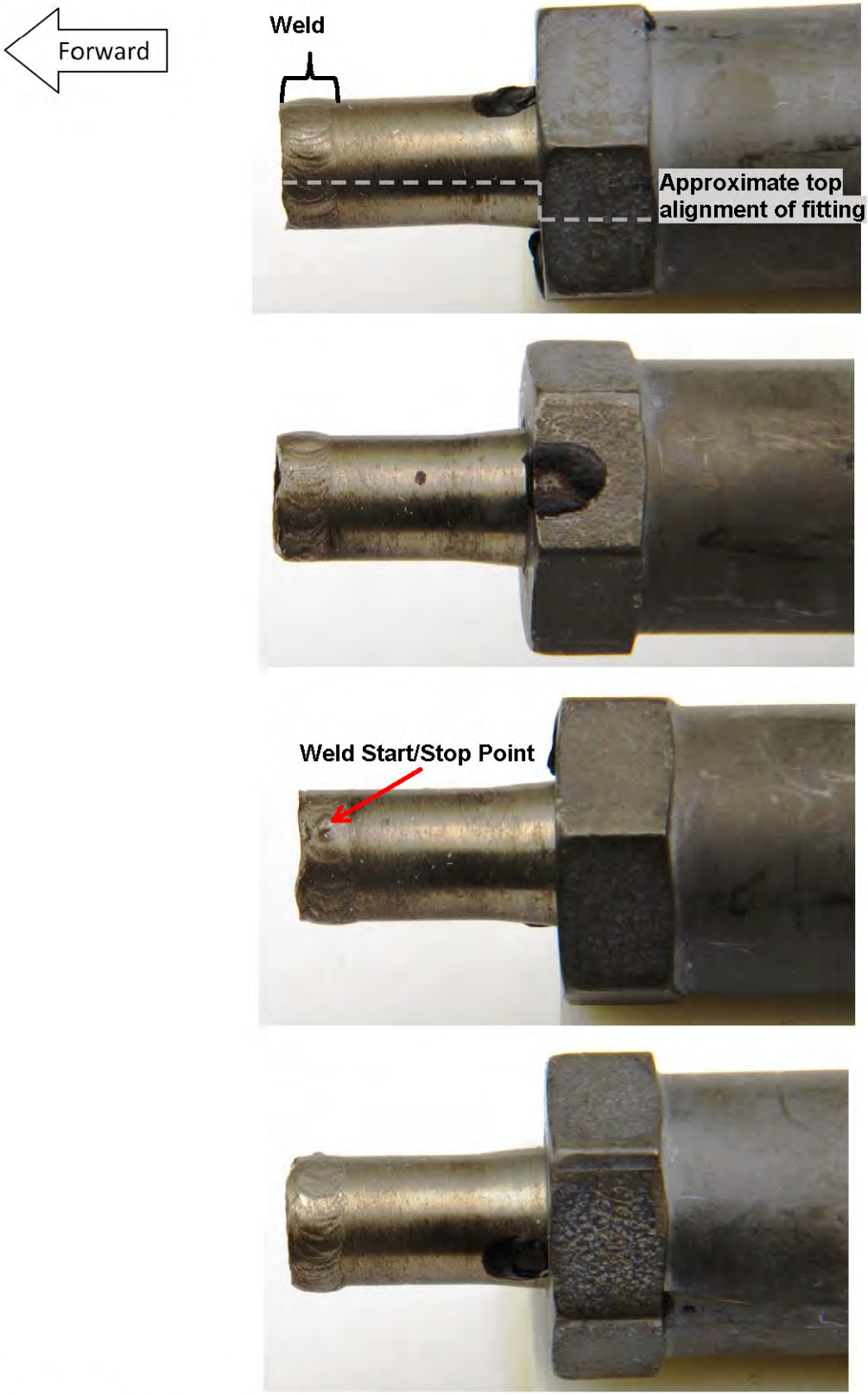

Figure 11. 90° rotated detailed views showing the weld and fitting side of the fractured tube. The fracture was at the toe of the weld on the side opposite the fitting. The tube was rotated 90° counterclockwise, forward looking aft, for this succession of images.

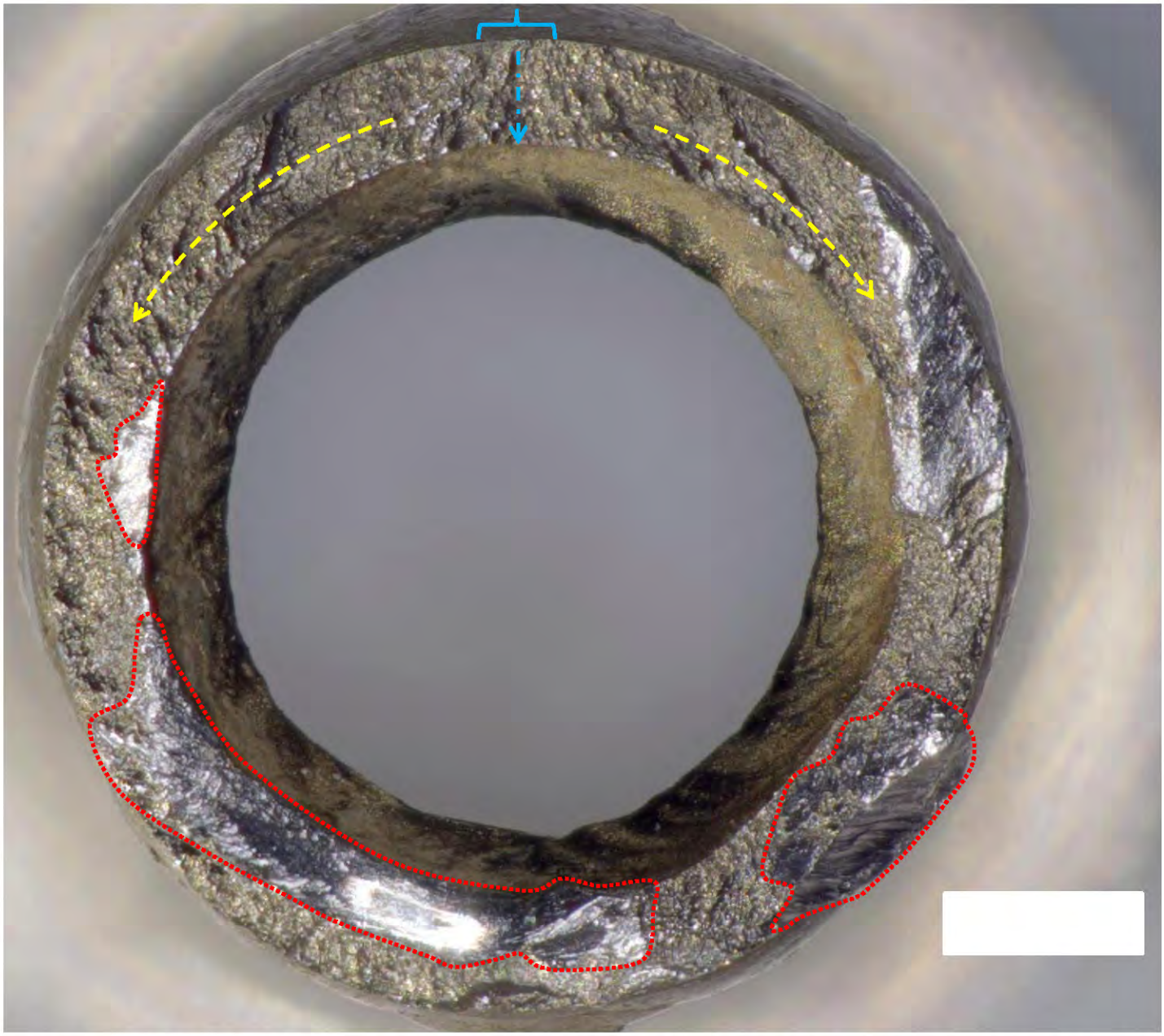

Figure 12. Detailed view showing the fitting side fracture surface after cleaning. The fracture features radiated from the outer diameter near the top directly through the thickness of the tube (blue brace and arrow), shown in Figure 14. The fracture features radiated away from the through-thickness fractured area around the circumference in both directions (yellow dashed arrows). The fracture exhibited smearing in several continuous areas around the circumference of the tube (red dashed outlined areas).

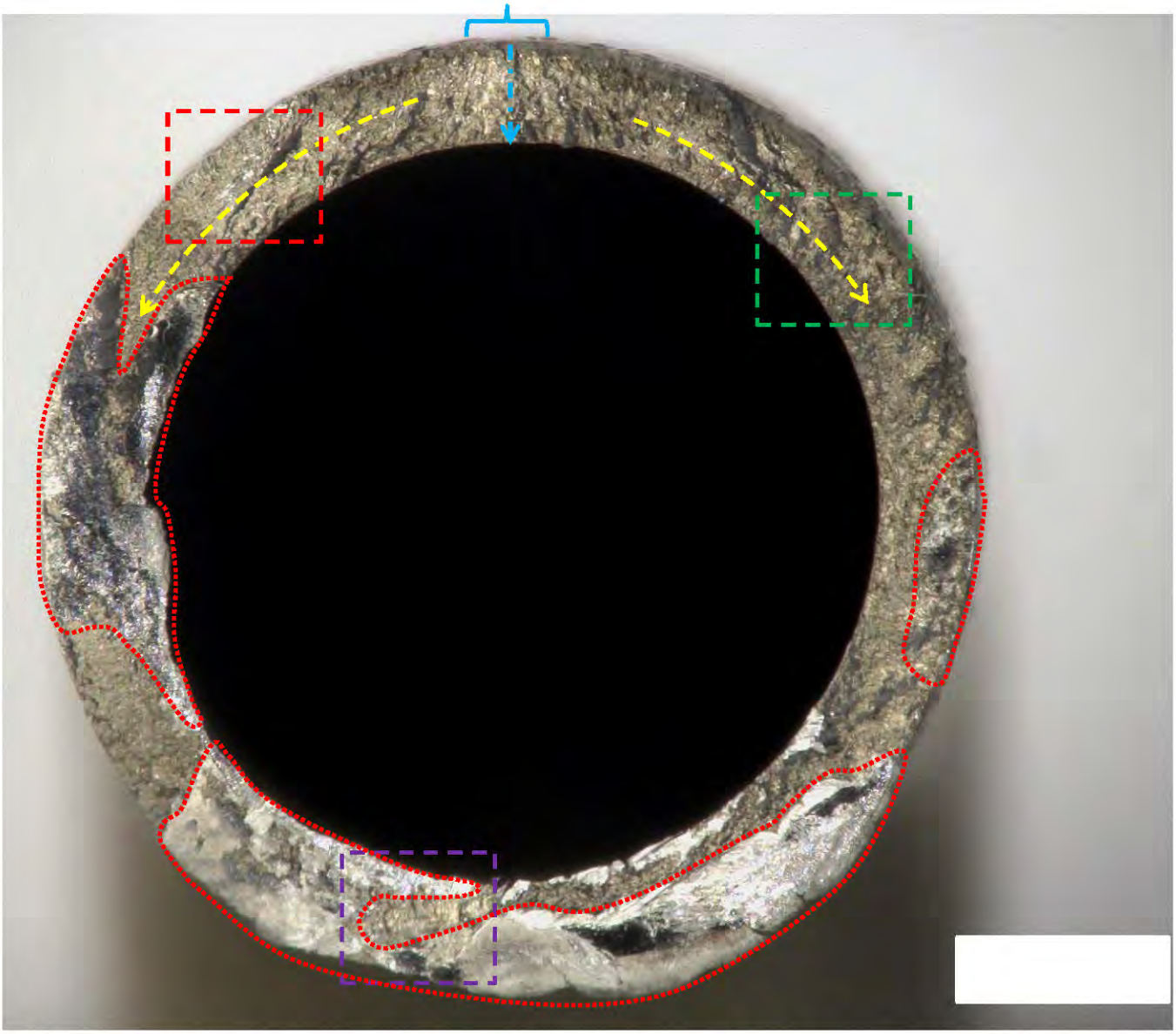

Figure 13. Detailed view showing the tube side fracture surface after cleaning. The fracture features radiated from the outer diameter near the top directly through the thickness of the tube (blue brace and arrow, through thickness fracture shown in Figure 16). The fracture features radiated away from the through-thickness fractured area around the circumference in both directions (yellow dashed arrows). The fracture exhibited smearing in several continuous areas around the circumference of the tube (red dashed outlined areas). The areas in the red, green, and purple dashed boxes are shown in Figure 17, Figure 18, and Figure 19, respectively.

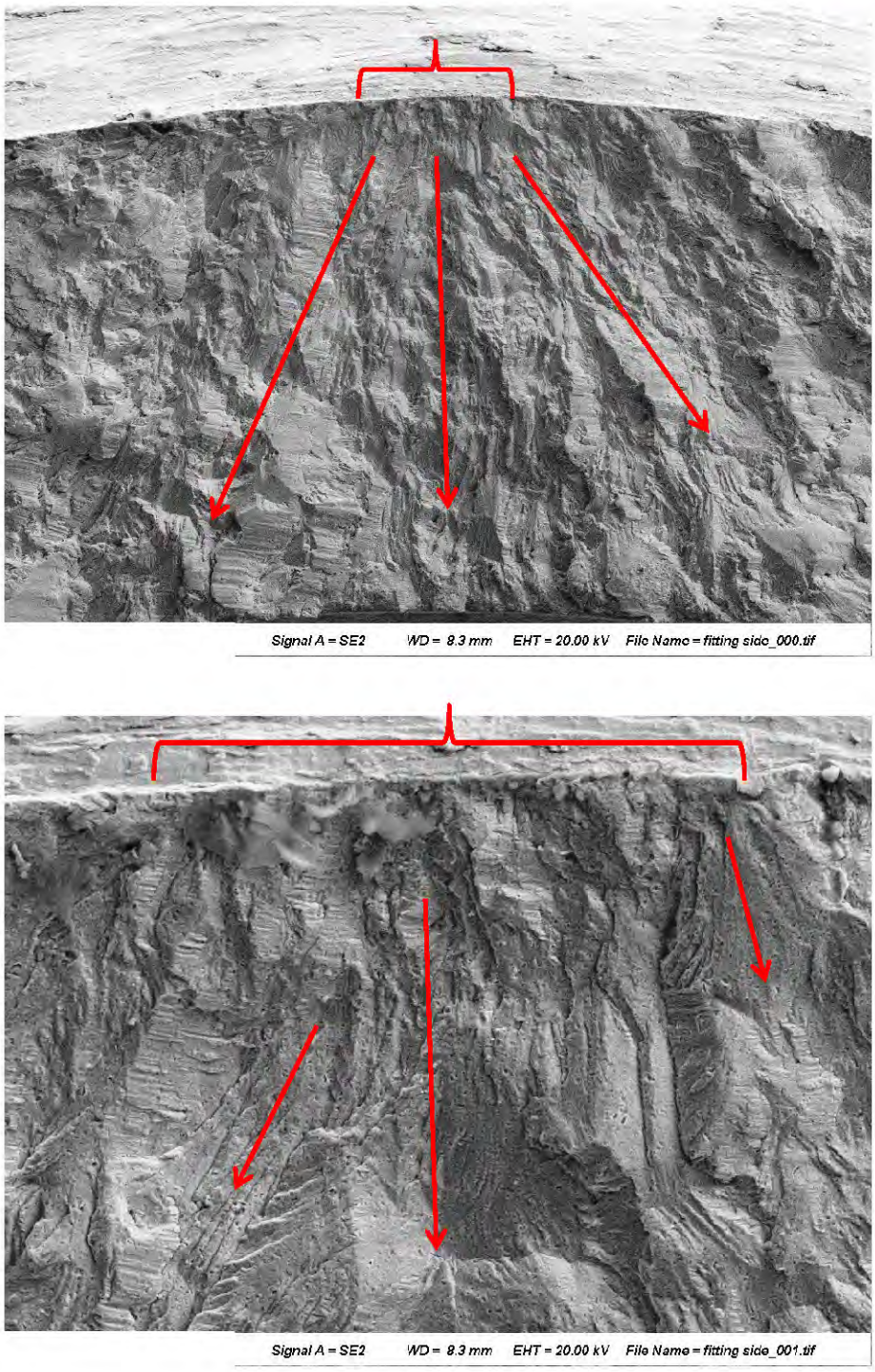

Figure 14. SEM images showing fracture features radiating away from the fatigue origin area (red brace) on the outer diameter surface near the top position of the tube on the fitting side of the fracture surface. Red arrows show the local direction of fatigue progression. Tilted views showing the outer diameter surface of the tube are shown in the following figure.

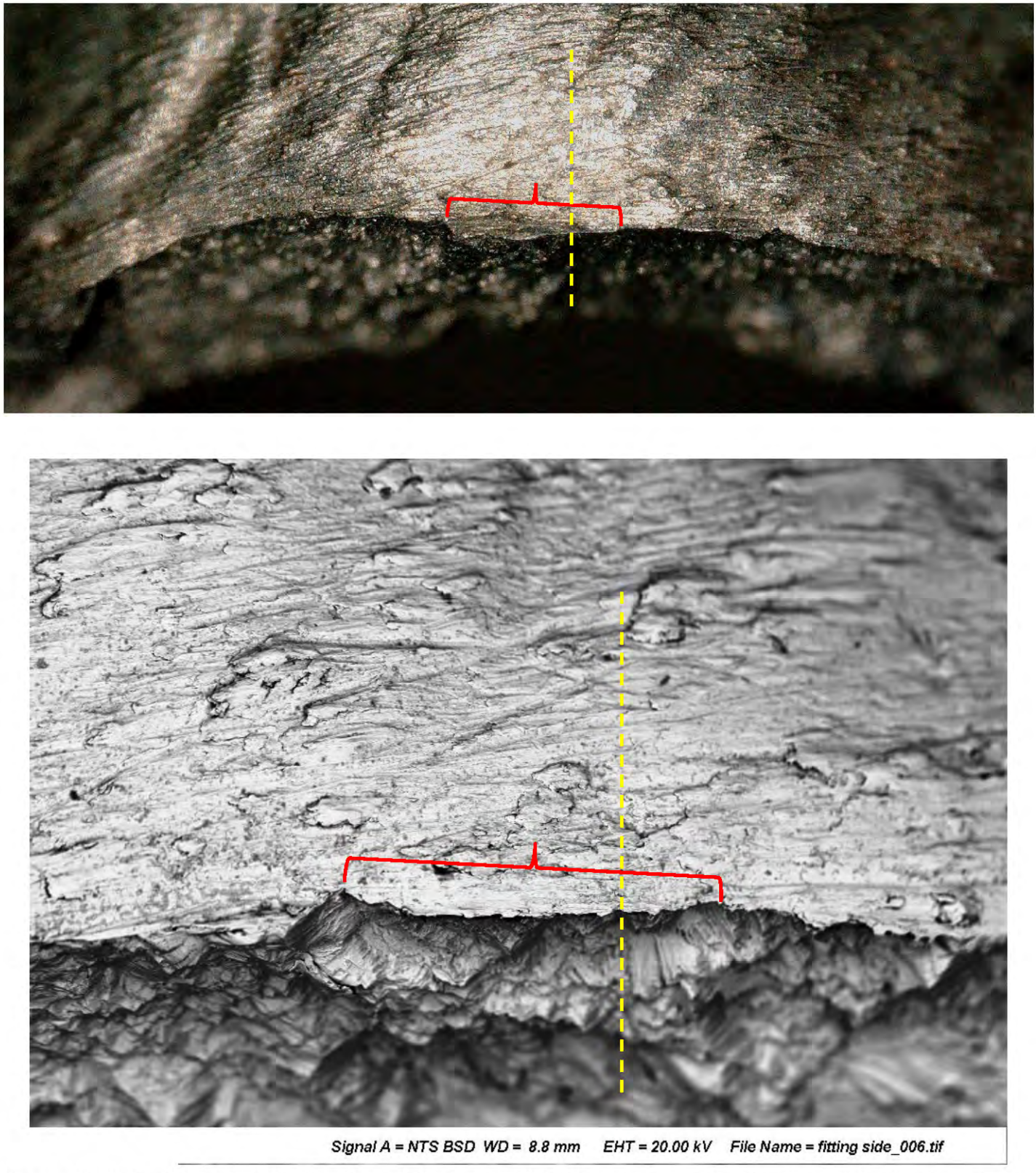

Figure 15. Optical (top) and backscattered electron SEM (bottom) images showing the weld outer diameter on the fitting side of the fracture surface adjacent to the origin area (red brace). The yellow dashed line shows the approximate plane of metallographic examination shown in Figure 22.

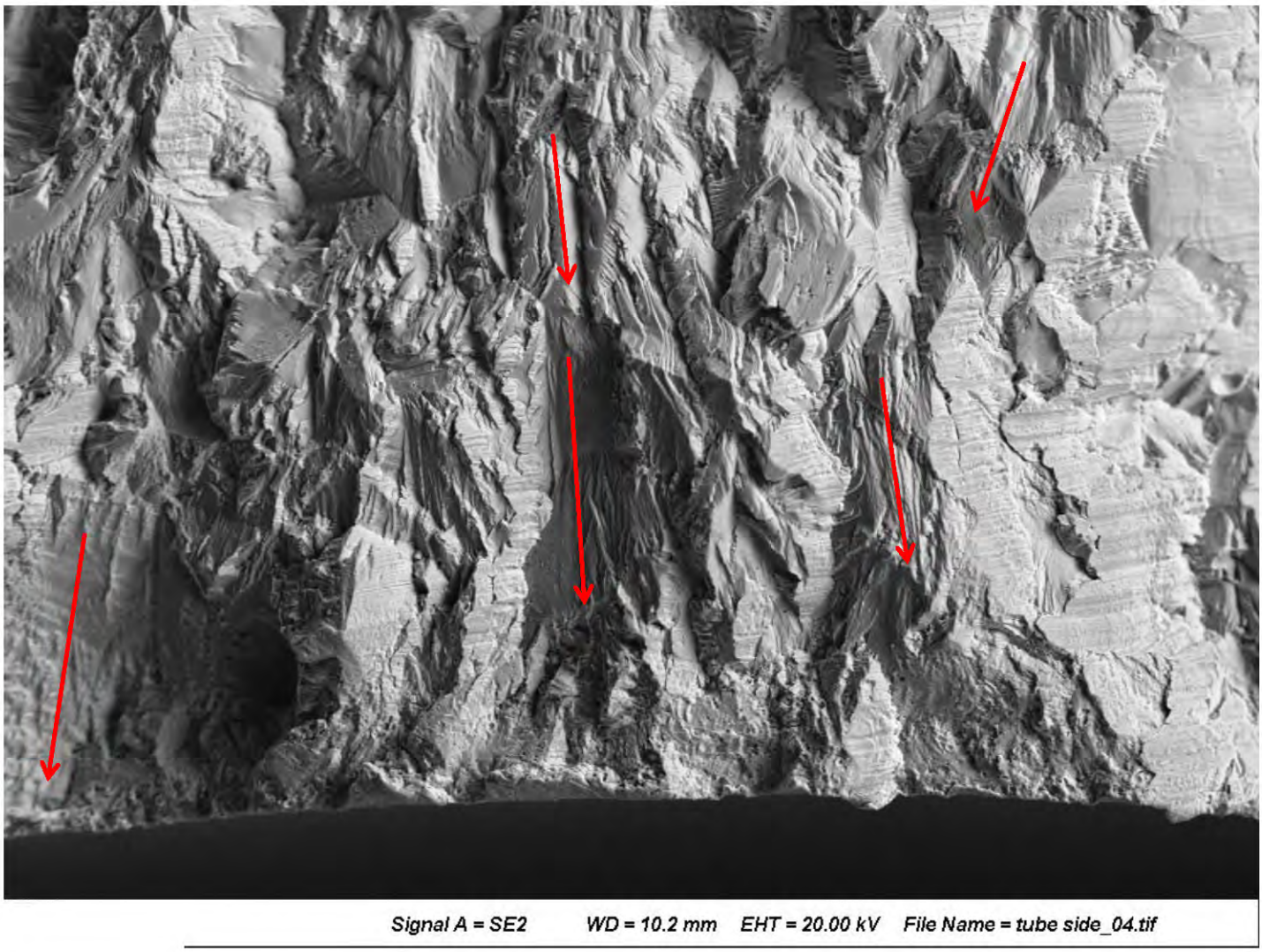

Figure 16. SEM image showing fatigue fracture features (red arrows) extending through the thickness of the tube on the tube side fracture surface.

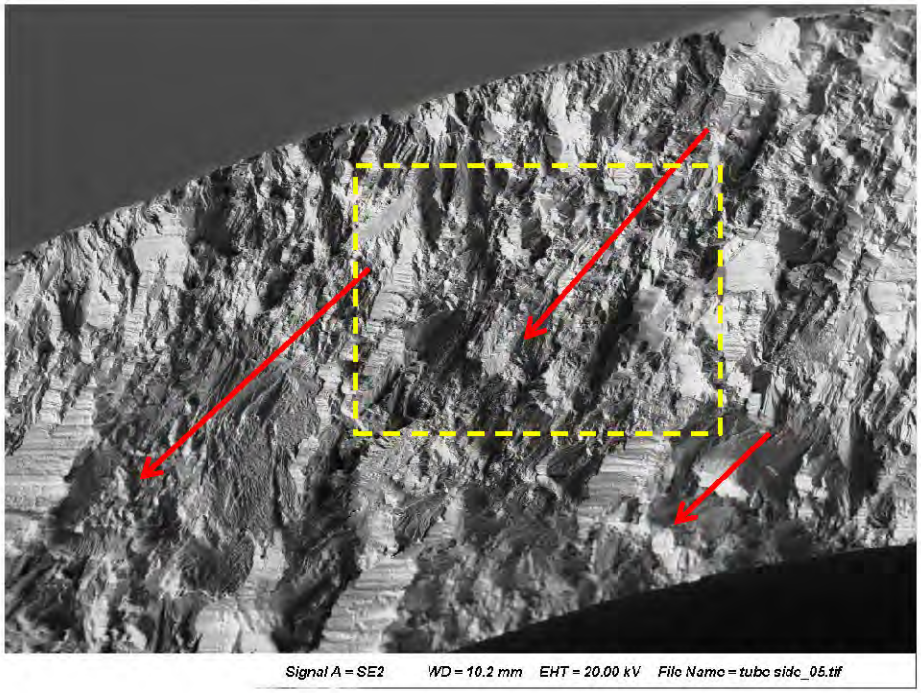

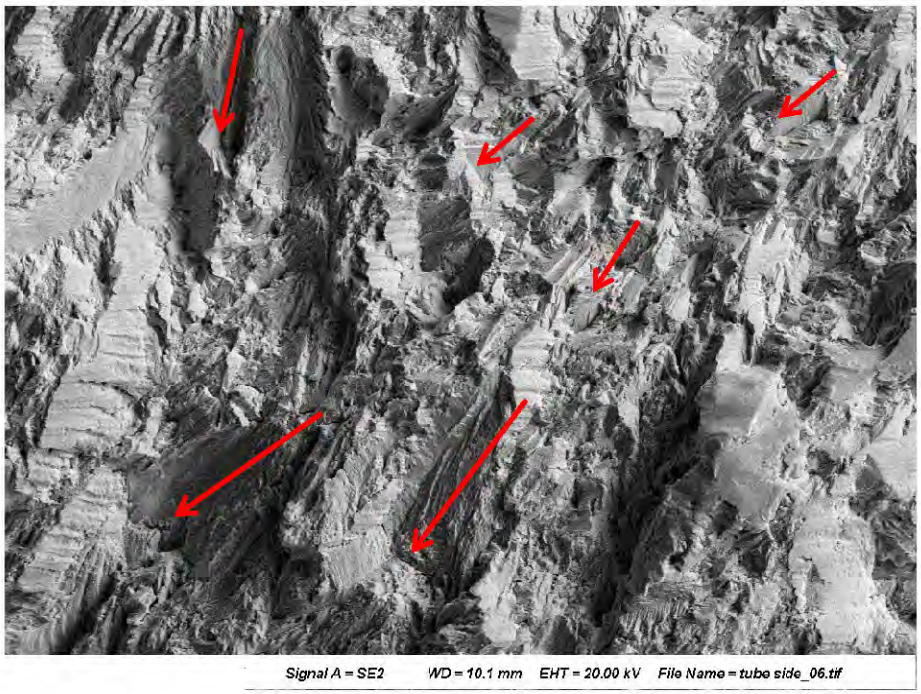

Figure 17. Representative fracture features consistent with fatigue progression counterclockwise circumferentially from the origin area on the tube side fracture surface. The fracture surface was intermittently smeared. Red arrows indicate the local direction of fatigue progression.

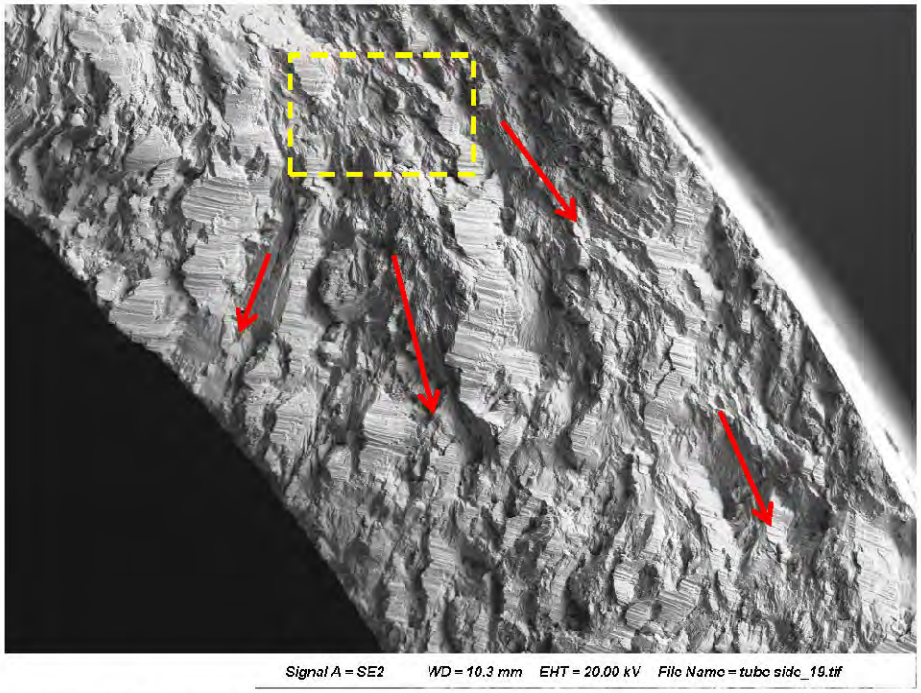

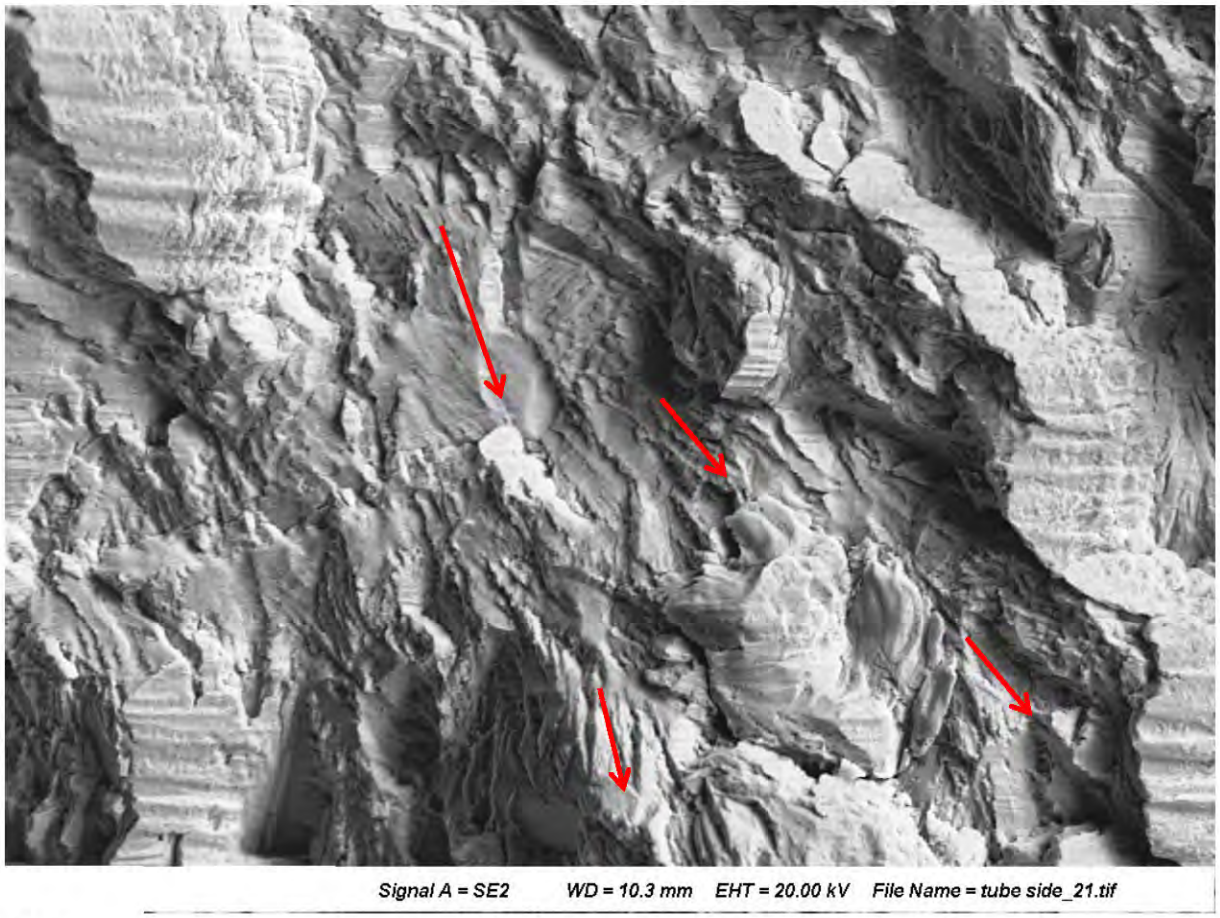

Figure 18. Representative fracture features consistent with fatigue progression clockwise circumferentially away from the origin area. The fracture surface was intermittently smeared. Red arrows indicate the local direction of fatigue progression.

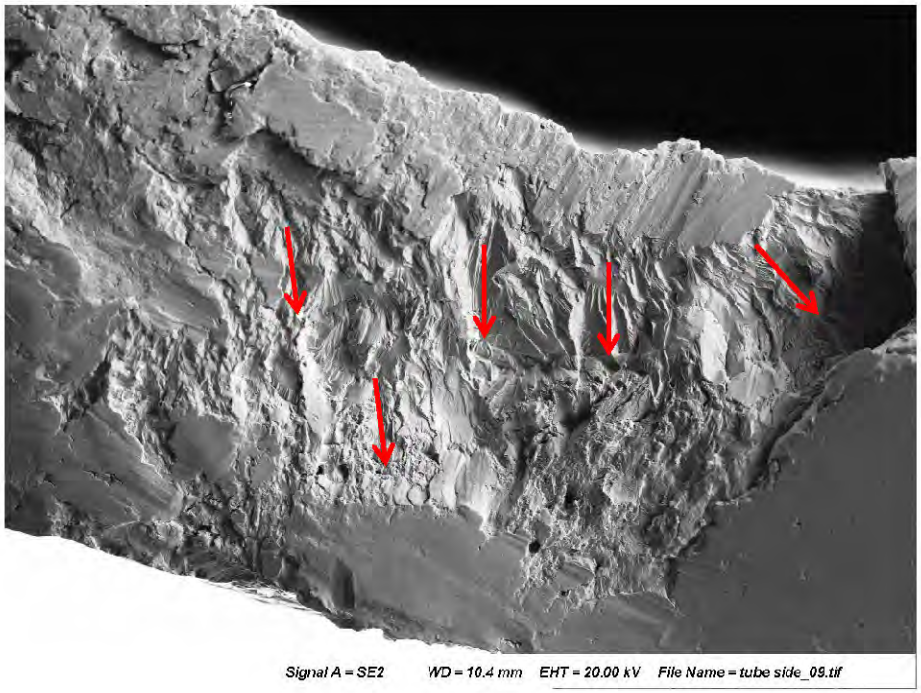

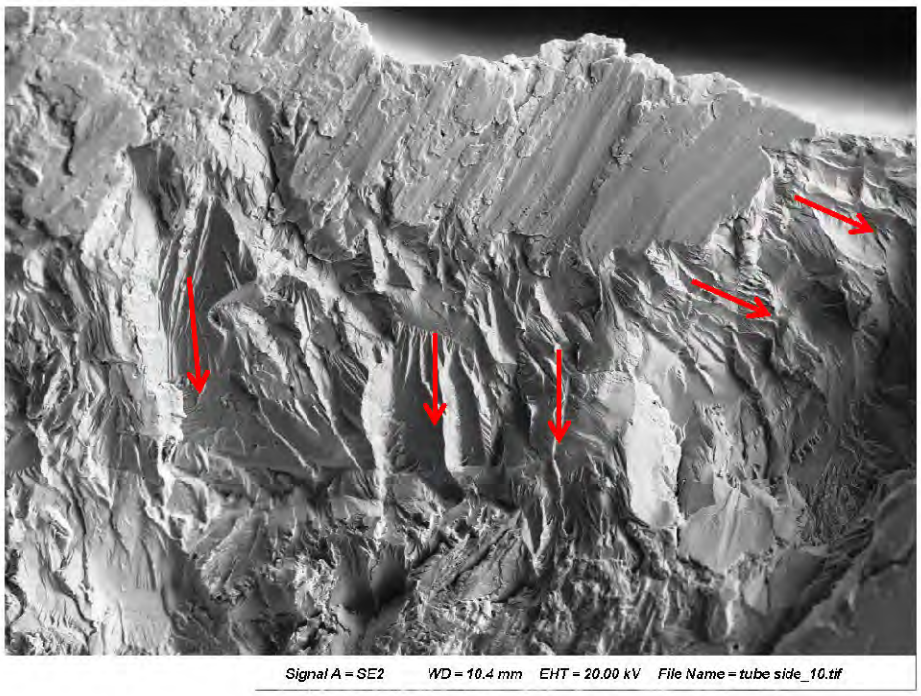

Figure 19. Fracture features consistent with fatigue progression emanating away from a smeared area adjacent to the inner diameter surface, approximately 200° clockwise from the origin. The red arrows show the local direction of fatigue progression.

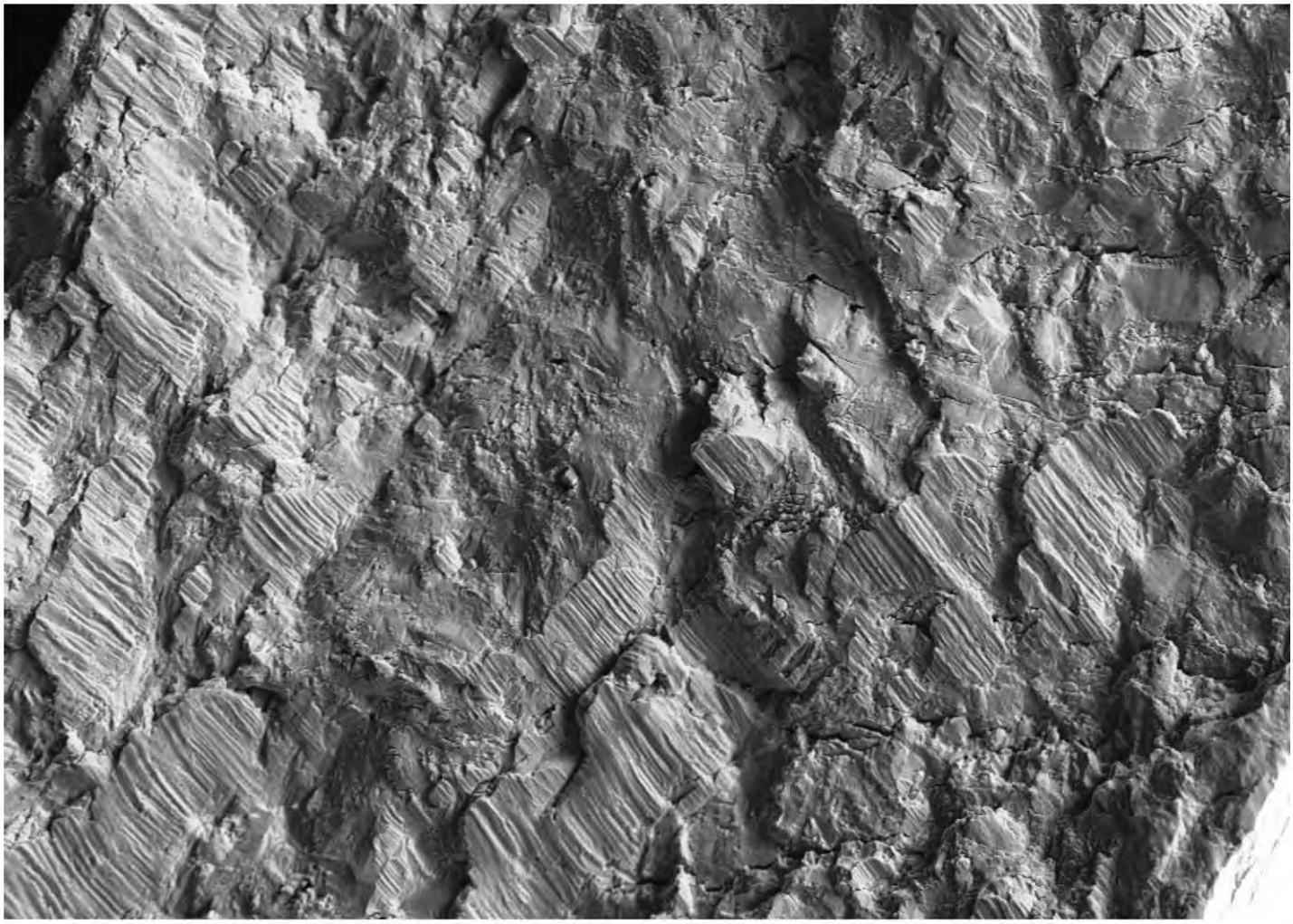

Figure 20. Detailed view of representative smearing damage located approximately 120° in the clockwise direction from the origin. The fracture surface spanning from approximately 120° to 200° clockwise from the origin was smeared and most of the fine fracture features were obliterated, precluding identification of the fracture mode.

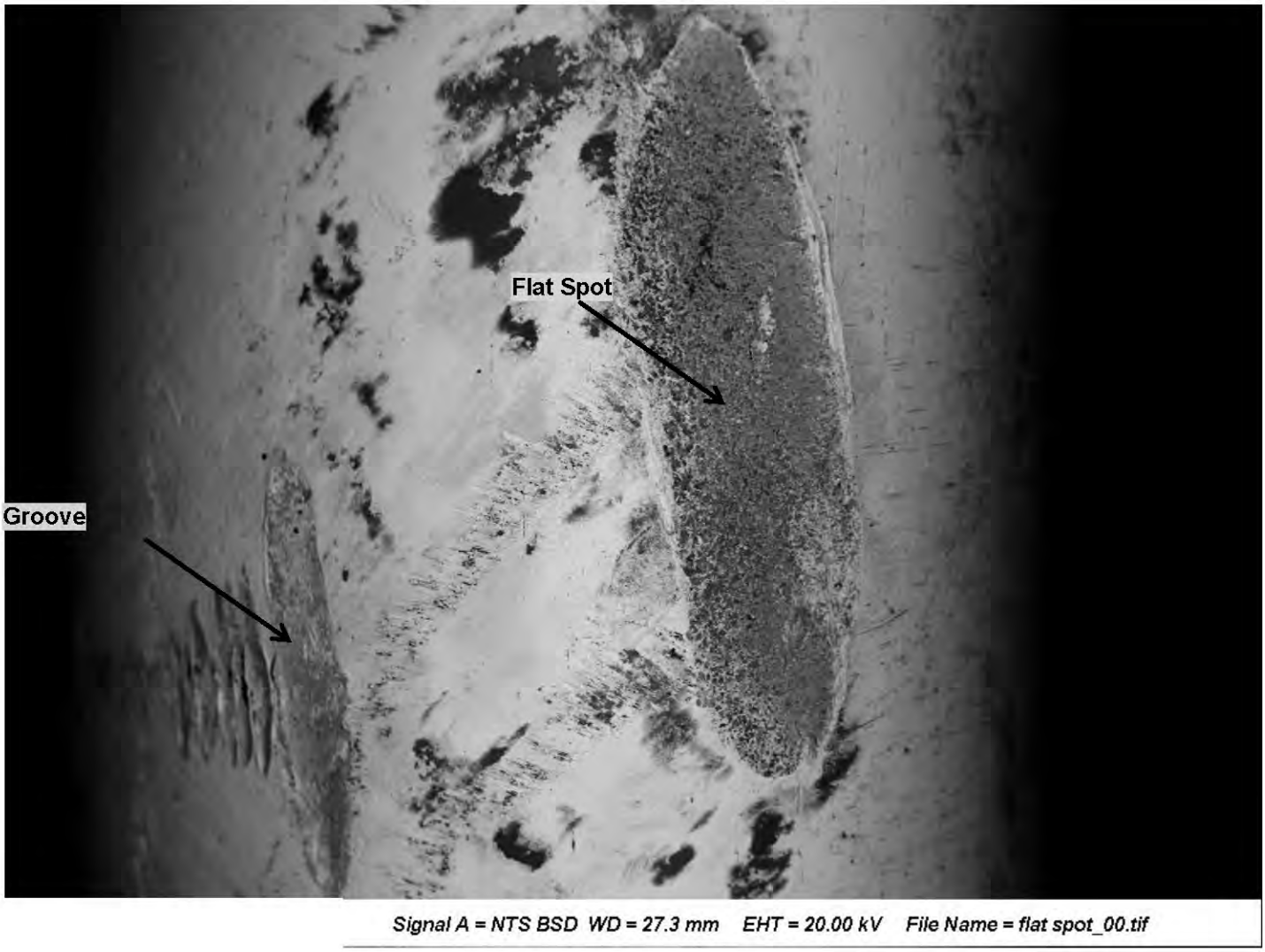

Element	Flat Spot (wt%)	Groove (wt%)
O	18.45	29.54
Si	6.03	1.54
Cr	2.59	3.94
Mn	0.54	0.66
Fe	68.32	62.9
Ni	1.02	1.43

Figure 21. Backscattered electron SEM image (top) showing the flat spot and adjacent parallel grooves. The table shows representative EDS results for the flat spot surface and largest groove. Arrows mark the test locations.

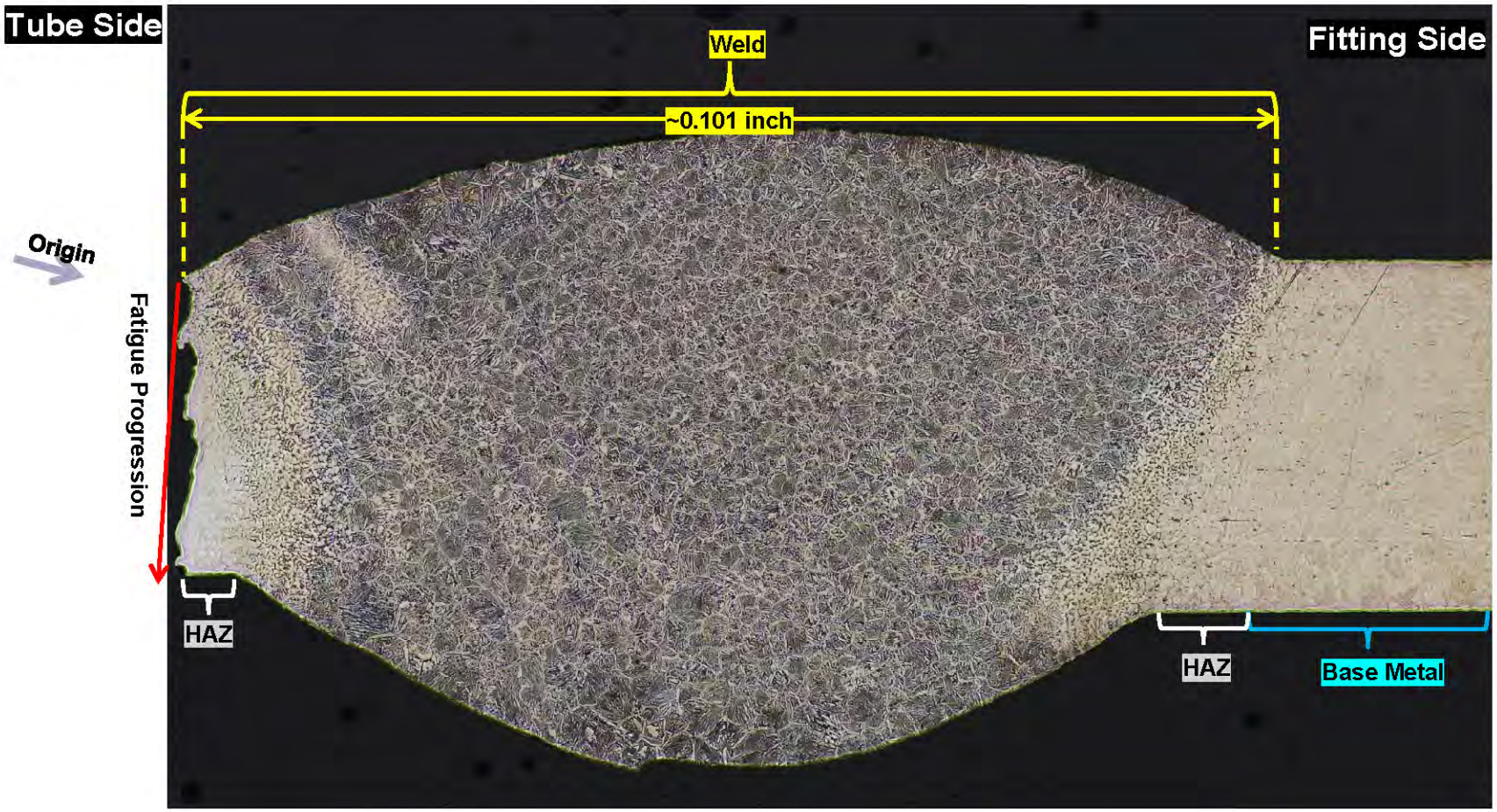

Figure 22. **Metallographic cross-section through the weld at the approximate plane of the fatigue origin area as indicated in Figure 15. The approximate areas of the weld (yellow brace), heat affected zone (HAZ; white braces), and base metal (blue braces) microstructures are annotated. The fracture origin (purple arrow) was at the approximate intersection between the HAZ and base metal microstructures on the tube side of the weld in this plane of examination. The red arrow shows the direction of fatigue progression. The fracture surface is shown in more detail in the following figure. Etchant: Stainless No. 2.**

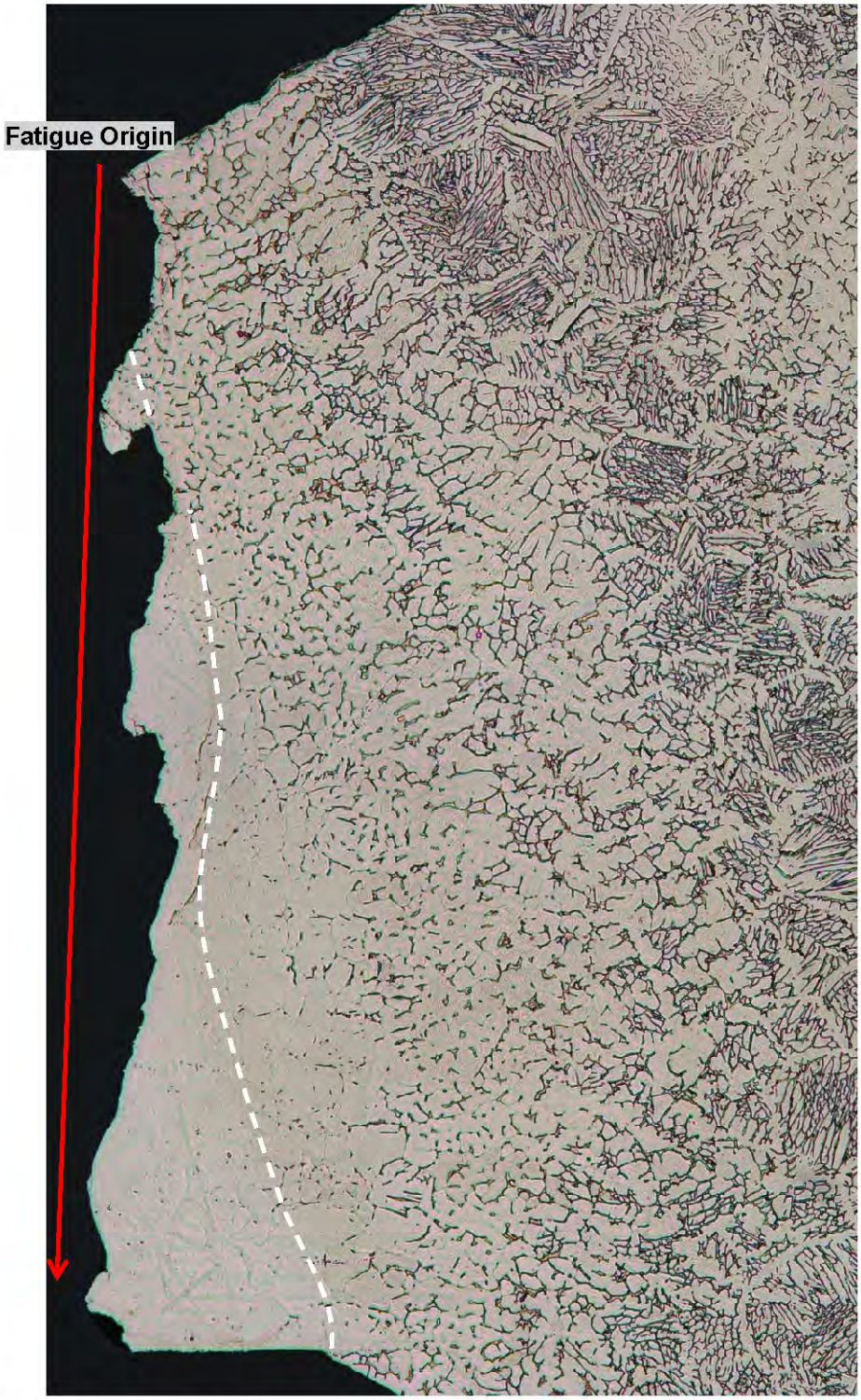

Figure 23. Detailed view showing the fatigue fracture surface on the cross-section shown in the previous figure. The red arrow shows the direction of fatigue progression through the thickness of the tube, initiating near the approximate transition between the HAZ and weld metal microstructures. The approximate transition between the HAZ and weld metal microstructures, where it was visually apparent in this plane of cross-section, is indicated by the white dashed line.
Etchant: Stainless No. 2.

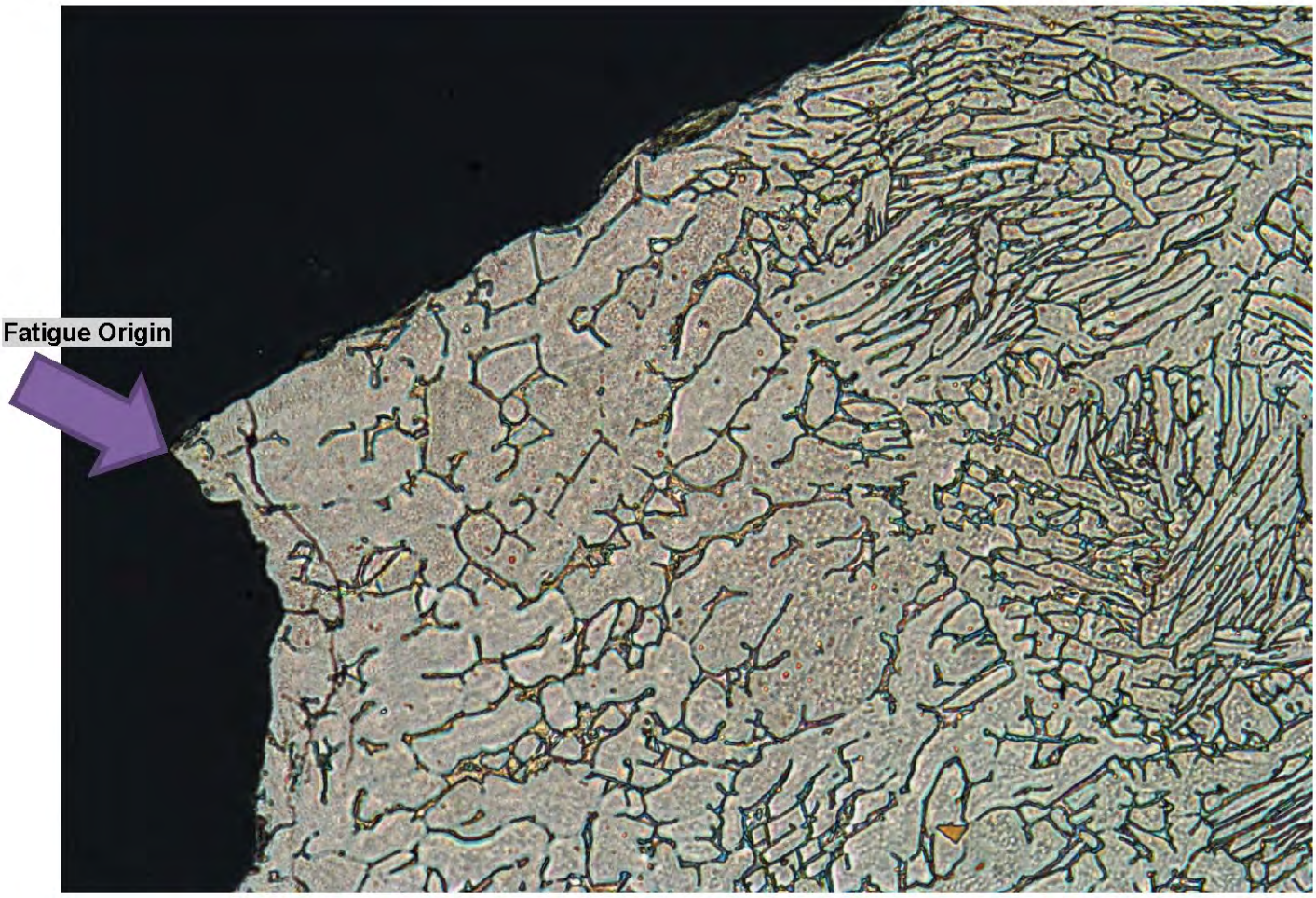

Figure 24. Detailed view of the fatigue origin area in cross-section. There were no material anomalies at the origin. Etchant: Stainless No. 2.

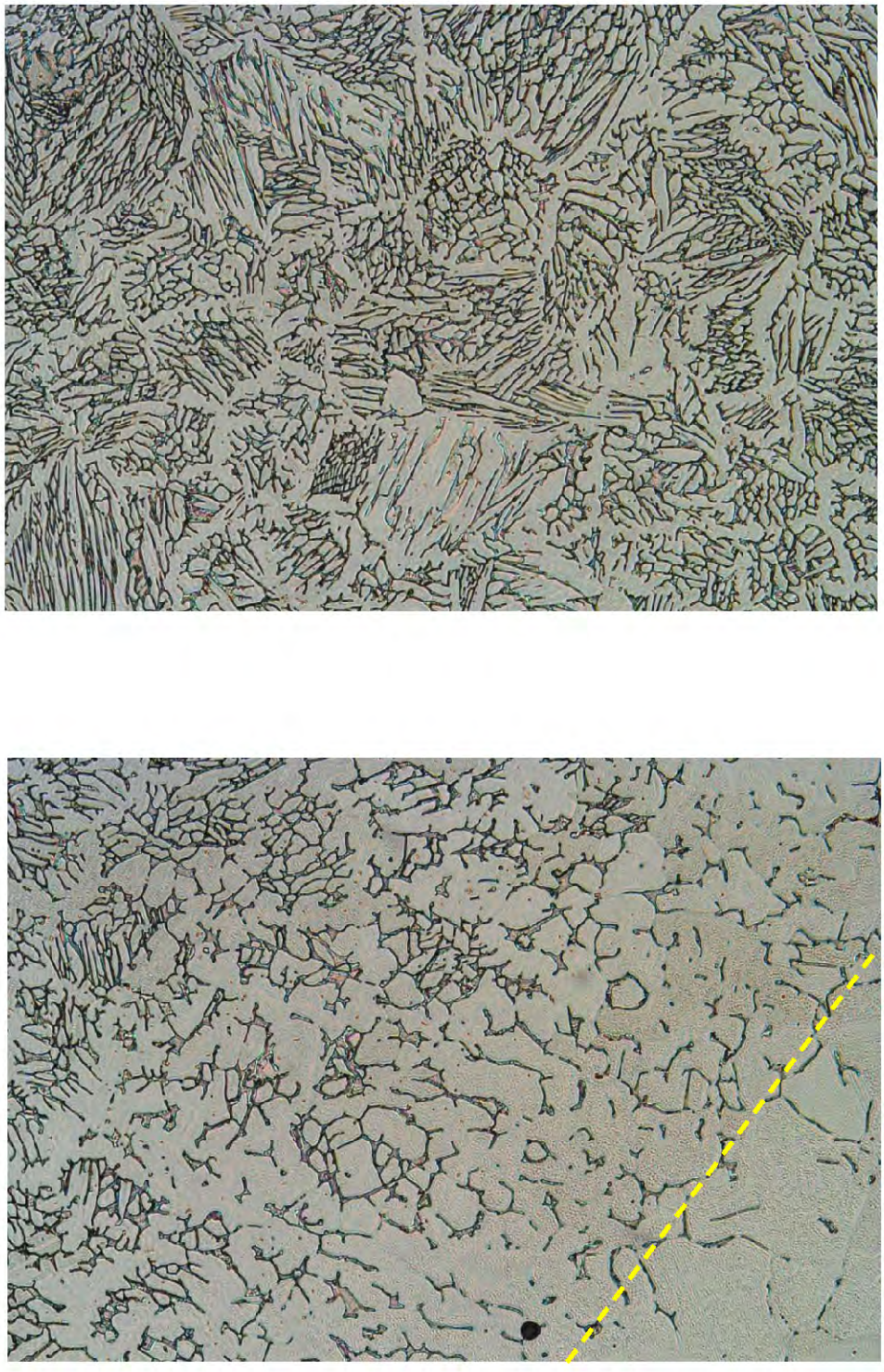

Figure 25. Detailed views showing the weld metal (above yellow dashed line) and HAZ (below yellow dashed line) microstructures found on the tube weld. Etchant: Stainless No. 2.

Figure 26. Detailed view showing the base metal microstructure. Etchant: Stainless No. 2.

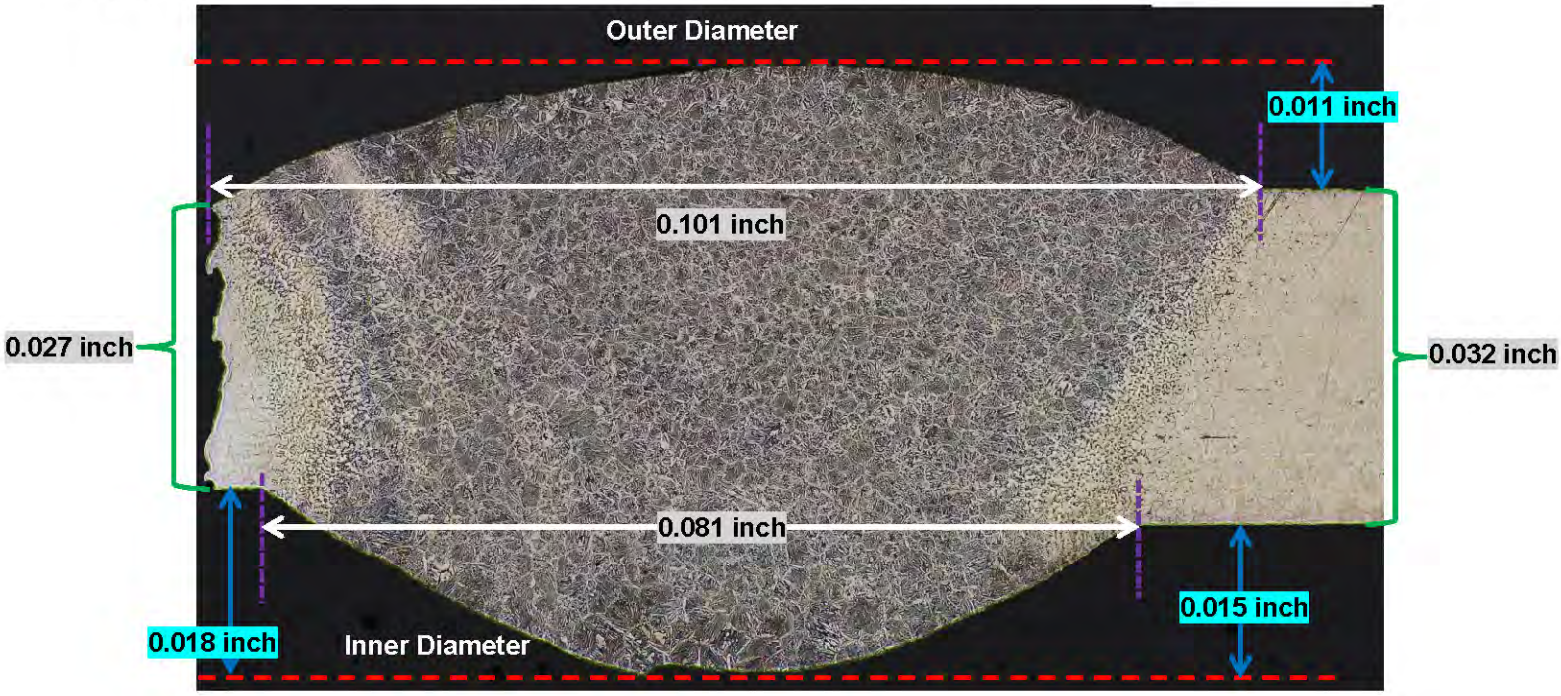

Figure 27. Overall view of the weld in cross-section annotated with the measured wall thicknesses of the tube and fitting (green braces) as well as the width (white arrows) and height (blue arrows) of the weld bead and root reinforcement at the plane of the fatigue origin. White arrows placed collinear with the inner and outer diameter surfaces of the fitting to illustrate the mismatching alignment of the tubes. Etchant: Stainless No. 2.

Figure 28. Overall view showing the cross-section through the flat spot (red brace) at plane 1 through the rub damaged area. In this plane of examination there was a slight concavity to the mostly flattened surface. There was no corresponding deformation of the inner diameter opposite the flattened area or material smeared from the flattened area onto the adjacent surface of the tube. Unetched.

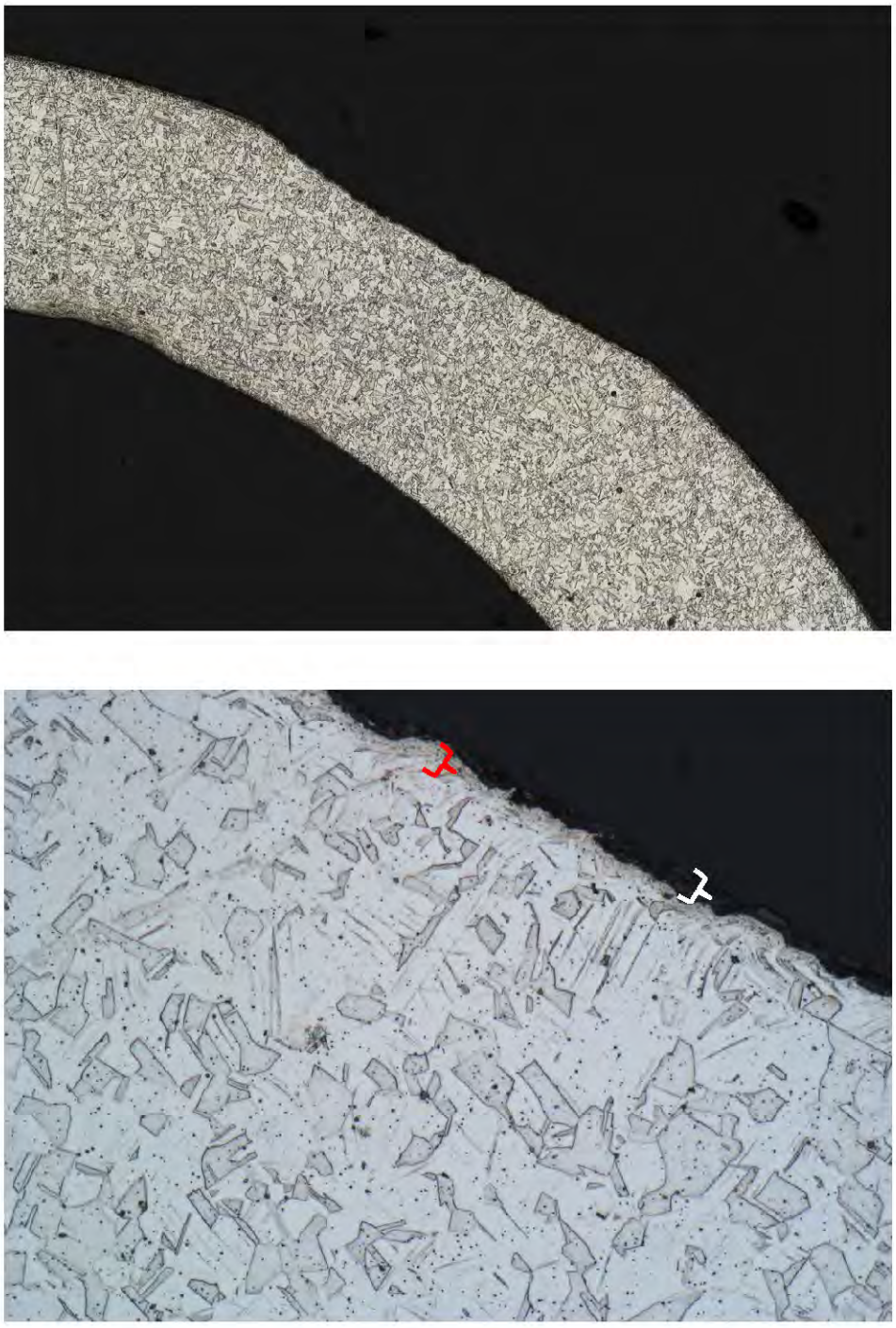

Figure 29. Detailed views showing the microstructure near the surface of the flat spot on plane 1. The flat spot had an oxide layer on the surface (white brace) under which the microstructure was distorted (red brace). Etchant: Stainless No. 2.

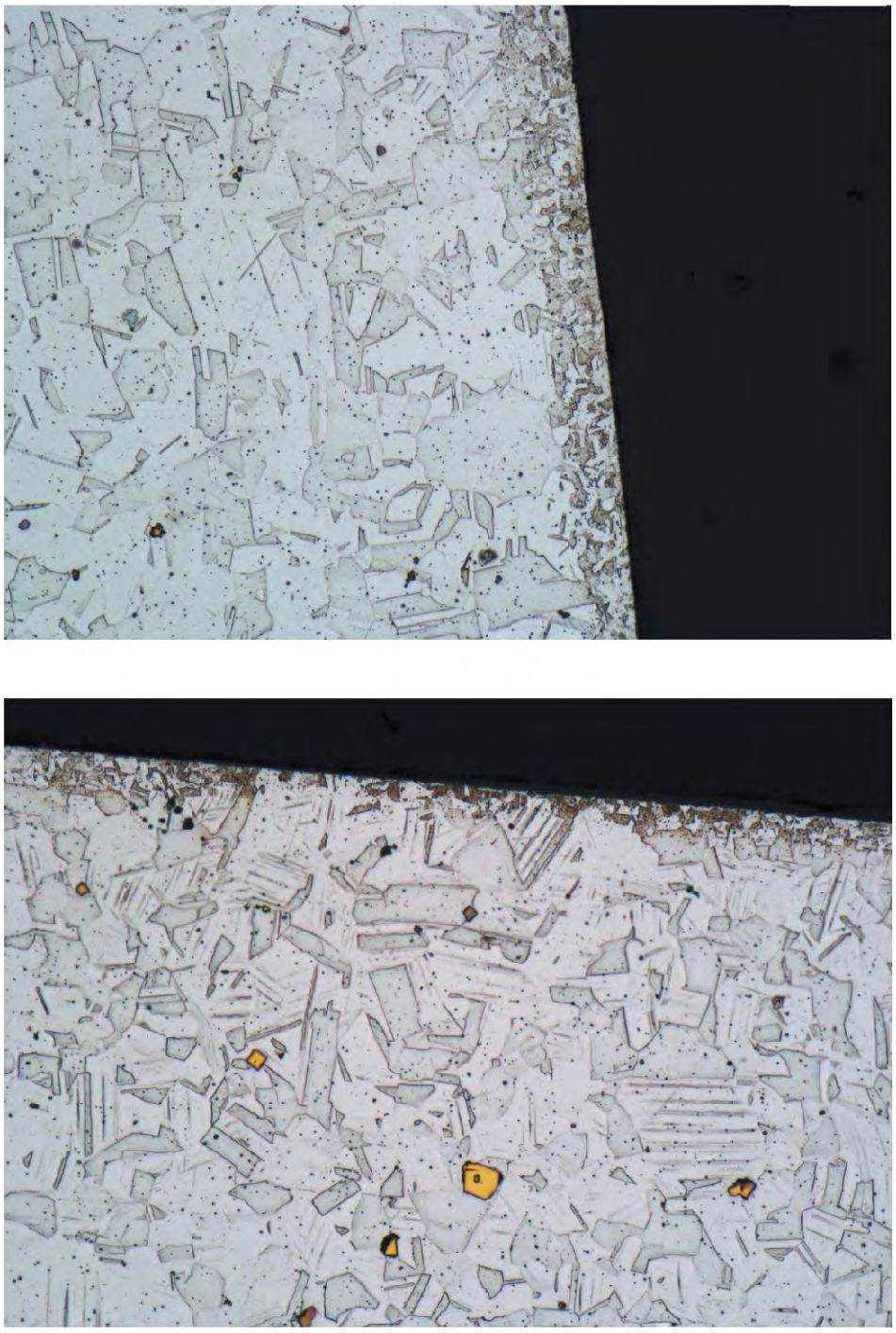

Figure 30. Detailed views showing representative surface microstructure away from the flattened area on plane 1. Etchant: Stainless No. 2.

Figure 31. Overall view showing the cross-section through the flat spot (red brace) and parallel grooves (blue brace) at plane 2 through the rub damaged area. In this plane of examination there was no curvature to the flat spot. There was no corresponding deformation of the inner diameter opposite the flattened area or oval-shaped darkened patches. Unetched.

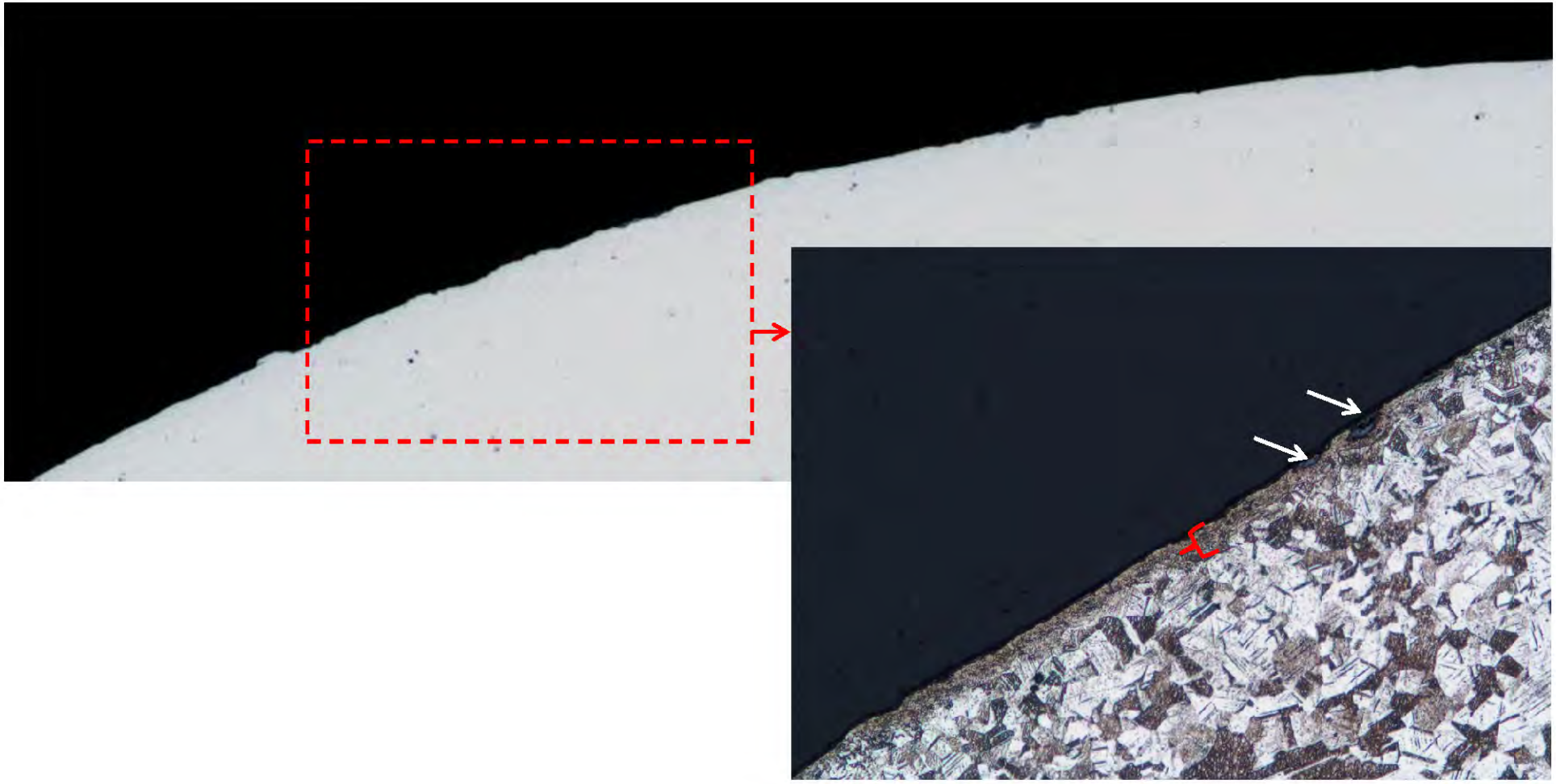

Figure 32. Overall view of the cross-section through the parallel grooves (top) and a detailed view of the representative microstructure at the surface of the grooves (inset). Some oxides were present on the surface (white arrows) and the microstructure was slightly distorted (red brace). Top: Unetched. Inset: Etchant: Stainless No. 2.